Original Research

Anti-Parkinson's evaluation of *Brassica juncea* leaf extract and underlying mechanism of its phytochemicals

Uzma Saleem[1,*], Shabana Bibi[2,3], Muhammad Ajmal Shah[4,*], Bashir Ahmad[5], Ammara Saleem[1], Zunera Chauhdary[1], Fareeha Anwar[5], Nimra Javaid[1], Sundas Hira[5], Muhammad Furqan Akhtar[5], Ghulam Mujtaba Shah[6], Muhammad Saad Khan[7], Haji Muhammad[8], Muhammad Qasim[9], Mohammad Alqarni[10], Majed A. Algarni[11], Renald Blundell[12,13], Celia Vargas-De-La-Cruz[14,15], Oscar Herrera-Calderon[14], Reem Hasaballah Alhasani[16]

[1]*Department of Pharmacology, Faculty of Pharmaceutical Sciences, Government College University, 38000 Faisalabad, Pakistan,* [2]*Yunnan Herbal Laboratory, College of Ecology and Environmental Sciences, Yunnan University, 650091 Kunming, Yunnan, China,* [3]*International Joint Research Center for Sustainable Utilization of CordycepsBioresouces in China and South-east Asia, Yunnan University, 650091 Kunming, Yunnan, China,* [4]*Department of Pharmacognosy, Faculty of Pharmaceutical Sciences, Government College University, 38000 Faisalabad, Pakistan,* [5]*Riphah Institute of Pharmaceutical Sciences, Riphah International University, 54000 Lahore, Pakistan,* [6]*Department of Botany, Faculty of Biological and Health Sciences, Hazara University, 21120 Mansehra, Pakistan,* [7]*Department of Biosciences, Faculty of Sciences, COMSATS University Islamabad, 57000 Sahiwal, Pakistan,* [8]*Department of Chemistry, Federal Urdu University of Arts, Science & Technology, 75300 Karachi, Pakistan,* [9]*Dr. Muhammad Ajmal Khan Institute of Sustainable Halophyte Utilization, University of Karachi, 75270 Karachi, Pakistan,* [10]*Department of Pharmaceutical Chemistry, College of Pharmacy, Taif University, 21944 Taif, Saudi Arabia,* [11]*Department of Clinical Pharmacy, College of Pharmacy, Taif University, 21944 Taif, Saudi Arabia,* [12]*Department of Physiology and Biochemistry, Faculty of Medicine and Surgery, University of Malta, MSD2080 Msida, Malta,* [13]*Centre for Molecular Medicine and Biobanking, University of Malta, MSD2080 Msida, Malta,* [14]*Department of Pharmacology, Bromatology, Toxicology, Faculty of Pharmacy and Biochemistry, Universidad Nacional Mayor de San Marcos, Jr. Puno 1002, 15001 Lima, Peru,* [15]*E-Health Research Center, Universidad de Ciencias y Humanidades, 15001 Lima, Peru,* [16]*Department of Biology, Faculty of Applied Science, Umm Al-Qura University, 21961 Makkah, Saudi Arabia*

TABLE OF CONTENTS

Submitted: 2 June 2021 Revised: 30 August 2021 Accepted: 26 October 2021 Published: ???

1. Abstract

Background: Parkinson's disease (PD) is associated with progressive neuronal damage and dysfunction. Oxidative stress helps to regulate neurodegenerative and neuronal dysfunction. Natural compounds could attenuate oxidative stress in a variety of neurological disorders. *B. juncea* is a rich source of antioxidants. The present study aimed to evaluate the therapeutic potential of *B. juncea* leaves for the treatment of PD by applying behavioral, *in vivo* and *in silico* studies. For *in vivo* studies rats were divided into six groups (n = 6). Group-I served as normal control (vehicle control). Group-II was disease control (haloperidol 1 mg/kg). Group-III was kept as a standard group (L-Dopa 100 mg/kg + carbidopa 25 mg/kg). Groups (IV–VI) were the treatment groups, receiving extract at 200-, 400- and 600 mg/kg doses respectively, for 21 days orally. **Results**: *In vivo* study results showed that the extract was found to improve muscles strength, motor coordination, and balance in PD. These behavioral outcomes were consistent with the recovery of endogenous antioxidant defence in biochemical analysis which was further corroborated with histopathological ameliorations. Dopamine levels increased and monoamine oxidase B (MAO-B) levels decreased dose-dependently in the brain during the study. Herein, we performed molecular docking analysis of the proposed extracted phytochemicals has explained that four putative phytochemicals (sinapic acid, rutin, ferulic acid, and caffeic acid) have presented very good results in terms of protein-ligand binding interactions as well as absorption, distribution, metabolism, excretion & toxicity (ADMET) profile estimations. **Conclusion**: The undertaken study concluded the anti-Parkinson activity of *B. juncea* and further suggests developments on its isolated compounds in PD therapeutics.

2. Introduction

Parkinson's disease (PD) is a severe neurologic dysfunction described by compromised motor coordination (postural imbalance, shaking, stiffness, loss of autonomic movements, and bradykinesia) and nonmotor symptoms (coherent defacement, disorganization, melancholy, reduced ability to detect the smell, hypersalivation, chewing and swallowing problems) [1–3]. It is considered the second most severe abnormality of the brain after Alzheimer's disease (AD). Patients with PD are reported about 2–3% after 65 years of age. Pathologically, it is a multifaceted disease with ambiguous etiology. Though gene mutation, environmental factors certain toxins (herbicide and pesticides), age and sex impart conclusive contribution in the disease etiology. Men are more prone towards this syndrome than women. It is ascribed to incessant dopaminergic neuronal loss in substantia nigra, lodgment of alpha-synuclein protein (Lewy bodies), neuronal inflammation, the damage of mitochondria along with oxidative stress. However, the cause for the deterioration of dopaminergic neurons is not well documented [4–6]. Glycation of α-synuclein is the main factor that leads to aggregation and formation of Lewy bodies, thus cause neuronal cell death in PD.

Up to date there is no curative therapy for PD. The available therapeutic options including levodopa, monoamine oxidase B inhibitors (MAO-B), beta-blockers, amantadine, and anticholinergics is not enough to treat the PD and associated organ demages [7, 8]. Moreover, there are a lot of adverse effects associated with the available therapies so that putative drugs and alternative cost-effective therapies are required with less or no adverse effects.

Several plant species and their secondary metabolites have been identified to possess excellent therapeutic potential against neurodegenerative disorders [9, 10]. Experimental and molecular mechanisms of natural PD inhibitors isolated from plants by experimental *in vitro* and *in vivo* analyses have been highlighted in several studies [10–12]. These plants have been found to exert a diverse range of protective effects that soothe devastating neurodegeneration. Generally, plant species with antioxidant properties have been widely recognized to ameliorate the disease process. For example, *Salvia Officinalis* possess rosmarinic acid, a potent free antioxidant that has been attributed to protecting the neurons from free radicals associated with cellular degeneration in AD and PD [13]. Certain herb families were found to regulate synaptic neurotransmission such as Ginseng [14, 15]. However, there is a long list of isolated bioactive compounds from medicinal plants that have been found to ameliorate neurodegenerative disorders [16–18].

Brassica juncea belongs to the family Cruciferae also called Indian mustard, mustard green, yellow mustard, black mustard [19]. The main planting nations are found in Asian countries. It is considered as a principal weed in Canada, Argentina, and Australia. Indian mustard was broadly dispersed also cultivated in subtropics regions and pleasant weather [20]. Previous studies suggested that *B. juncea* leaves are traditionally used as stimulants, diuretics, and expectorants and also as a food [21, 22]. Its seeds lubricant is mostly used as a traditional spice, for arthritis, foot ache, and rheumatism [23, 24]. *B. juncea* is an economically important edible plant [25]. The mustard plant is famous for its important components such as vitamin A, vitamin C, iron, calcium, selenium, chromium, and zinc supplements [26]. *B. juncea* contains a high proportion of alkenyl glucosinolates (85–96%) with the majority of sinigrin contents [27]. Phenyl isothiocyanate, phenolic compounds, fatty acids, glycosides, flavonoid, and proteins contents are present in this plant [21]. This plant contains phenolic and flavonoid compounds which have antioxidant and free radical scavenging activity [21]. Previous literature

has highlighted the importance of *B. juncea* leaves for various diseases, but the purpose of this study was to examine the therapeutic potential of *B. juncea* leaves and their secondary metabolites by the experimental evaluation with respect to high performance liquid chromatography (HPLC), physicochemical, quantitative, *in vitro* and *in vivo* studies. Moreover, molecular docking simulations assisted to validate the binding interactions of the selected metabolites within the catalytic cleft of enzyme acetyl cholinesterase (AChE) whose binding site was already determined and studied for drug design and development study. Significant binding energies in terms of Kcal/mol and binding interactions of the functional residues of AChE target active site with atoms of the selected metabolites could lead towards the novel drug development for the treatment of PD, and that might be significant for the treatment of several other brain diseases because AChE is a renowned molecular target for neurodegenerative diseases. *In silico* pharmacokinetics and toxicity prediction are the prerequisite of drug design studies and could be helpful for the initial screening of drug-like parameters of the selected metabolites, which could highlight major issues of the drug to be chemically improved in future before moving towards the drug development clinical studies. Findings of this experimental and computational analysis will add knowledge, and motivates the neuroscience researcher towards the advanced methodologies in future for the novel PD drug development.

3. Results

3.1 HPLC, physiochemical analysis, and quantitative phytochemical analysis of leaves powder

The physicochemical analysis of *B. juncea* leaves powder revealed that the loss on drying was 2.60% thus moisture content was found to be within the hygroscopicity range limit. It contained total ash contents of 4.55%, water-soluble ash 1.05%, acid insoluble ash 3.60%, alcohol soluble contents 9.42%, water-soluble contents 1.05%. The alcohol and water contents of the plant revealed an aqueous-alcoholic cosolvent with advanced extractive capacity and purity while sulfated ash was found to be 5.1 % contents.

Alkaloid contents of *B. juncea* extract were estimated by the linear regression equation y = 0.0009x (R^2 = 0.9748) which was obtained by drawing a graph between concentration versus absorbance. The extract of *B. juncea* contained 42.66 μg atropine equivalent/mg of alkaloids. The phenolic contents were determined by the mean of linear regression equation y = 0.0014x (R^2 = 0.9764) which was obtained by drawing a graph between concentration versus absorbance. The extract contained 107 μg gallic acid equivalent/mg of contents. The contents of flavonoids were estimated by the linear regression equation y = 0.0009x (R^2 = 0.9711) which was obtained by drawing a graph between concentration versus absorbance. The plant extract contained 4 μg quercetin standard equivalent/mg of contents. In Fig. 1, the standard curves were demonstrated.

Table 1. Phytochemicals identified in the *B. juncea* leaves extract in HPLC analysis.

S. no	Compounds	Retention time (min)	Quantity (mg/g extract)
1	Pyrogallol	13.63	1.38
2	Gallic acid	14.46	1.42
3	Catechol	17.63	25.34
4	Catechin	19.99	5.04
5	Hydroxybenzoic acid	21.39	23.84
6	Chlorogenic acid	23.98	6.42
7	Caffeic acid	26.90	3.63
8	Sinapic acid	27.55	2.41
9	Coumaric acid	33.13	0.22
10	Ferulic acid	34.44	0.49
11	Rutin	40.52	12.47

Eleven compounds were identified and quantified in the HPLC. The compounds in the increasing order of quantity (mg/g extract) are catechol (25.34) > hydroxybenzoic acid (23.84) > rutin (12.47) > chlorogenic acid (6.42) > catechin (5.04) > caffeic acid (3.63) > sinapic acid (2.41) > gallic acid (1.42) > pyrogallol (1.38) > ferulic acid (0.49) > coumaric acid (0.22) (Fig. 2, Table 1).

3.2 In vitro antioxidant potential

The 2,2-diphenyl-1-picrylhydrazyl (DPPH) scavenging assay was used to assess the antioxidant potential of plant extract at various concentrations. The percentage radical scavenging activity of the plant extract was increased dose-dependently. The maximum %age scavenging was presented by plant extract at 1000 μg/mL (70%) which was notably varied from ascorbic acid (56%). The IC_{50}value ofextract and ascorbic acid were calculated using linear regression equation was y = 0.0.0253x (R^2 = 0.9232) and y = 0.0.0338x (R^2 = 0.9272) respectively. The IC_{50}valueof extract was137.54 μg/mL while the IC_{50} value of ascorbic acid was 159.85 μg/mL.

3.3 Evaluation of anti-Parkinson's activity

3.3.1 Behavioral studies

The catalepsy in haloperidol-induced PD ~~in~~ rats was determined by employing block, hang and triple horizontal bar tests. The catalepsy timing was significantly ($p < 0.001$) rose in the DCG as compared to the NCG in the block test (Fig. 3A). The plant extract at 200, 400, and 600 mg/kg dosage had expressed a significant ($p < 0.001$) reduction in the level of catalepsy on the 7th, 14th, and 21st day of study as compared to the DCG on respective days. Hang test and horizontal bar timing were significantly ($p < 0.001$) decreased in the DCG in comparison to the NCG (Fig. 3B,C). The diseased rats treated with the plant extract at 200, and 400 mg/kg showed a significant ($p < 0.001$) rise in the timing in hang as well as horizontal bar test on the 7th, 14th, and 21st day of study as compared to that of DCG on

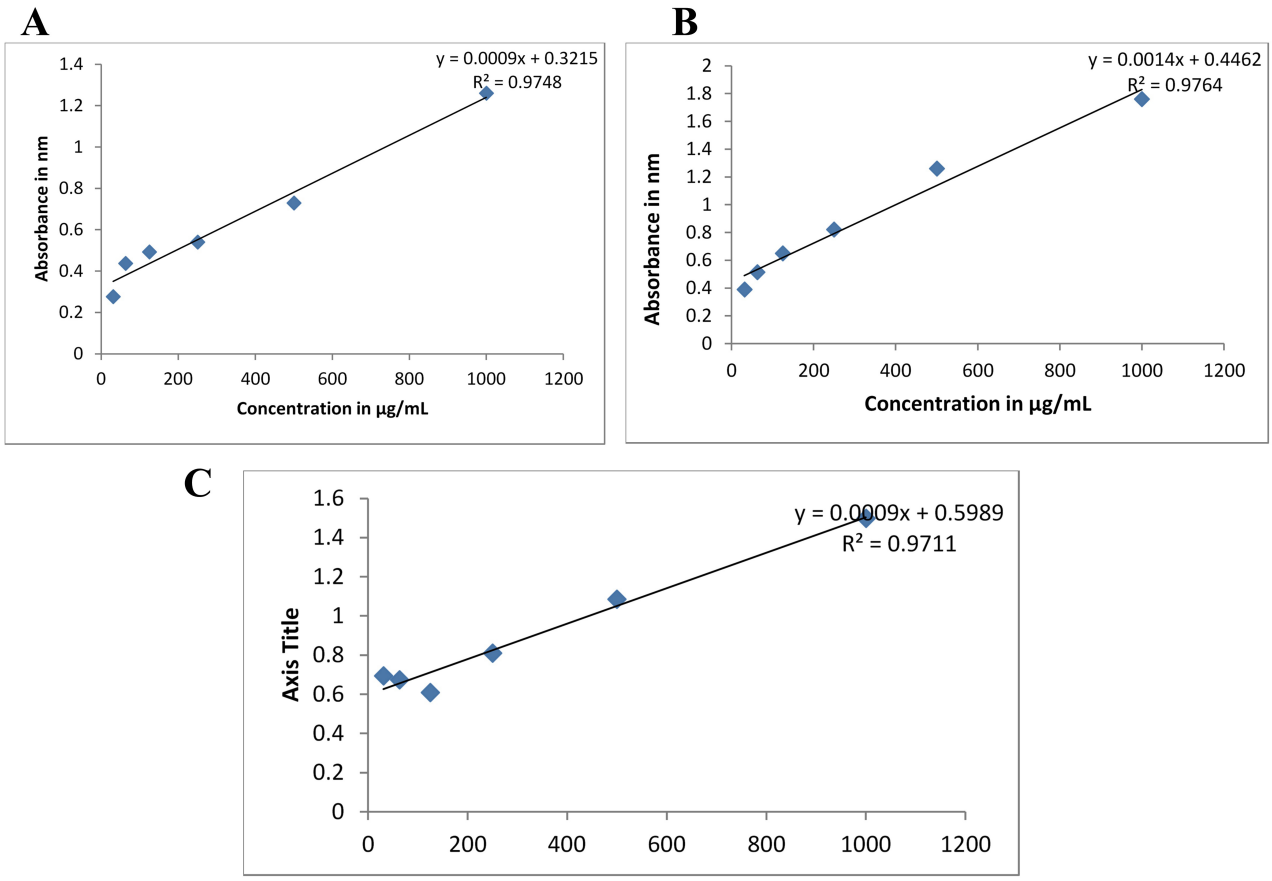

Fig. 1. The standard curve of atropine (A), gallic acid (B) and quercetin (C). y = y-intercept, x = x-intercept, R^2 = coefficient of determination.

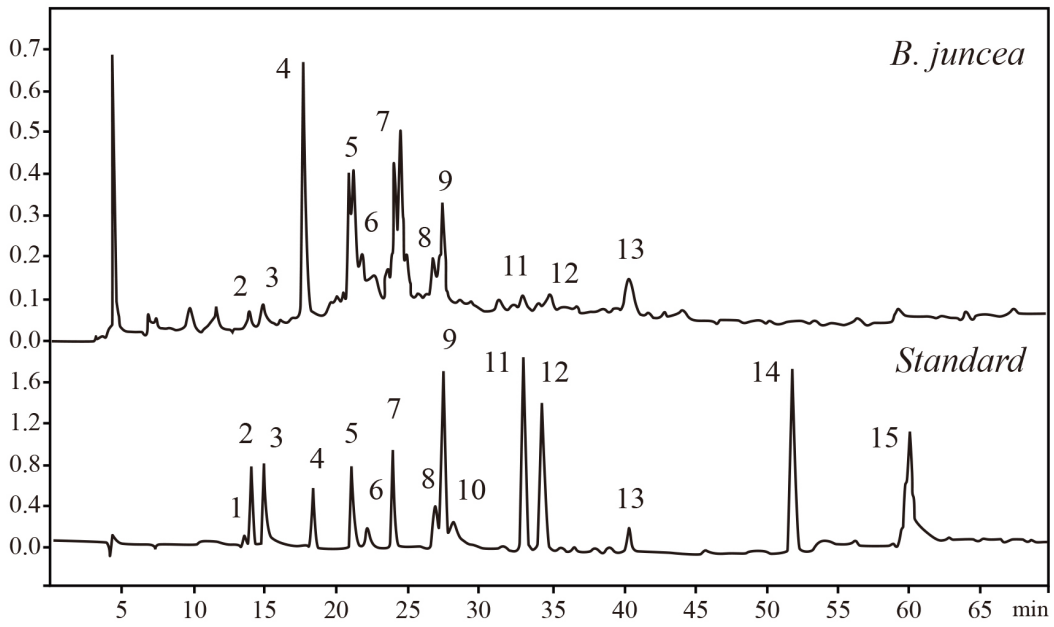

Fig. 2. HPLC chromatogram of *B. juncea* leaves extract and its standard phenolic compounds.

a respective day. Horizontal bar and hang bar timing was increased in a dose-dependent manner as the dose increased the time to stay in the horizontal bar test was also increased.

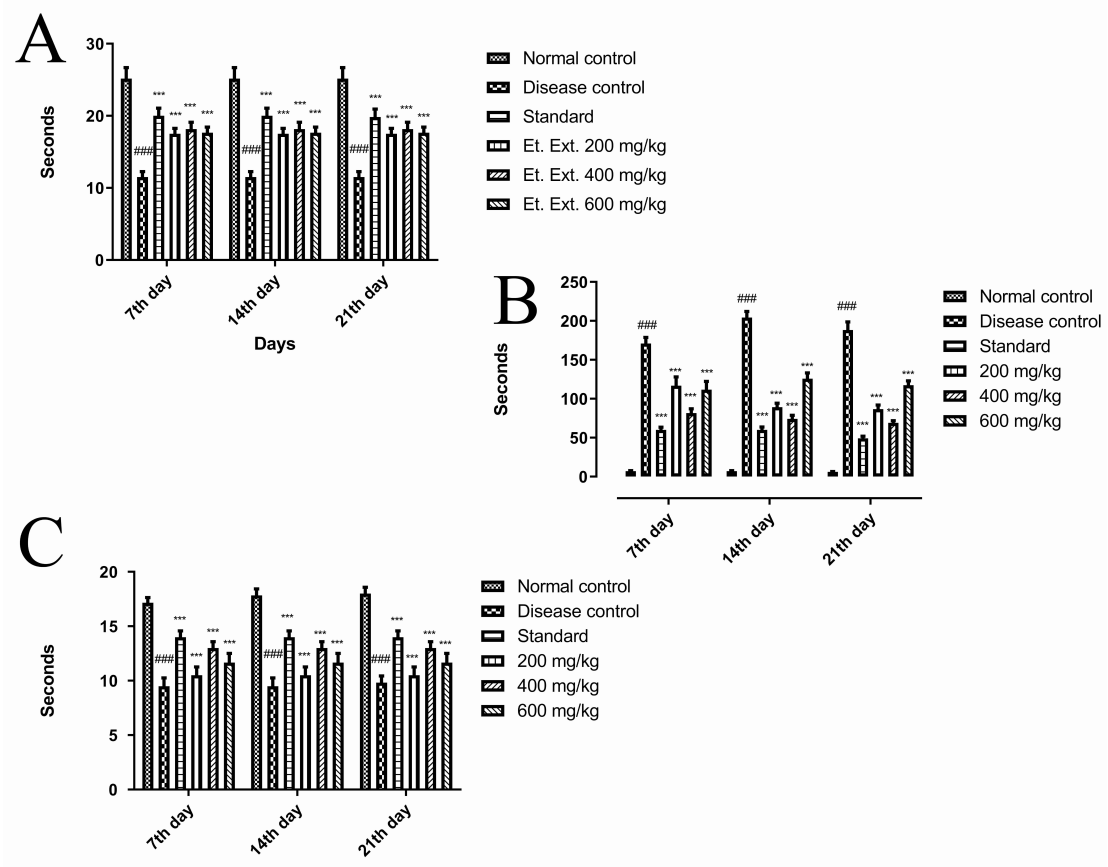

Fig. 3. Effect of *B. juncea* extract on catalepsy in haloperidol induced Parkinsonism in rats using block test (A), Hang test (B) and Horizontal bar (C). $^{###}p < 0.001$ vs normal control, $^{***}p < 0.001$ vs disease control.

3.3.2 Effect of B. juncea extract on oxidative stress biomarkers in brain and liver

The SOD, CAT, and GSH levels were significantly decreased with an increase in the MDA levels in the DCG as compared to the NCG. SOD, CAT, and GSH levels were increased significantly in the groups treated with the *B. juncea* extract. The extract showed maximum effect at 600 mg/kg (Table 2).

3.3.3 Effect of B. juncea extract treatments on dopamine levels

As shown in Fig. 4, the level of dopamine was significantly ($p < 0.001$) raised in the animals treated with the *B. Juncea* extract at different dose levels when compared with the disease control. A dose-dependent increase in the levels of dopamine was observed in the animals treated with *B. juncea*.

3.3.4 Effect of B. juncea extract treatments on MAO-B levels

As shown in Fig. 5, *B. juncea* at 600 mg/kg dose level significantly reduced the levels of MAO-B in the brain of the treated animals when compared with the disease control. However, other doses also showed a decrease but it was non-significant when compared with disease control.

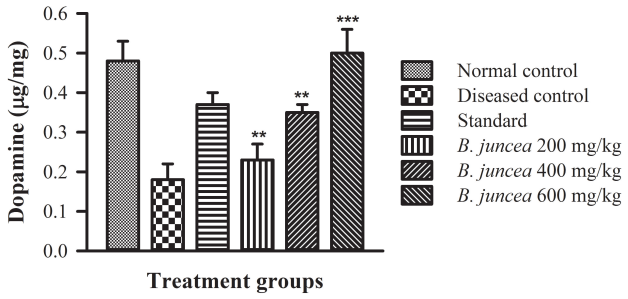

Fig. 4. Effect of *B. juncea* extract on dopamine levels in rat model. $^{**}p < 0.01$ & $^{***}p < 0.001$ as compared to the disease control.

3.3.5 Histopathological examination of brain tissue

The histopathological study of brain tissue of DCG revealed an increase in vacuolated cytoplasm (i.e., lipid peroxidation) and depletion of dopaminergic neurons. The NCG brain slide showed no vacuolated cytoplasm and as well as no depletion in dopaminergic neurons. The standard group revealed significant recovery from cytoplasmic vacuolation and dopaminergic neurons (Fig. 6C). However, the extract 200 mg/kg treated rat's brain showed moderate recovery from vacuolation and dopaminergic neurons while extract-treated groups at 400 and 600 mg/kg exhib-

Table 2. Effect of *B. juncea* extract on oxidative stress biomarkers in tissue homogenates in Haloperidol induced Parkinsonism in rats.

Groups	Doses	SOD (µg/g)	Catalase (mg/g)	GSH (µg/mg)	MDA (µmole/mgof protein)
Normal control (Vehicle)	1 mL/kg	6.362 ± 0.007	548.337 ± 0.007	1.807 ± 0.003	173.143 ± 0.012
Disease control (Haloperidol)	1 mg/kg	3.928 ± 0.006$^{###}$	398.810 ± 0.005$^{###}$	0.747 ± 0.004$^{###}$	309.755 ± 0.008$^{###}$
Standard (L-Dopa + Carbidopa)	100 mg/kg + 25 mg/kg	5.725 ± 0.002***	484.460 ± 0.010***	1.268 ± 0.005***	210.675 ± 0.005***
Extract	200 mg/kg	5.167 ± 0.003***	401.067 ± 0.007***	1.078 ± 0.005***	310.017 ± 0.004**
	400 mg/kg	5.353 ± 0.003***	424.958 ± 0.008***	1.160 ± 0.004***	263.262 ± 0.011***
	600 mg/kg	6.315 ± 0.004***	430.665 ± 0.010***	1.218 ± 0.003***	241.955 ± 0.011***

The values are expressed as mean ± SEM, (n = 6). ###$p < 0.001$ vs. normal control. ***$p < 0.001$ vs. disease control group.

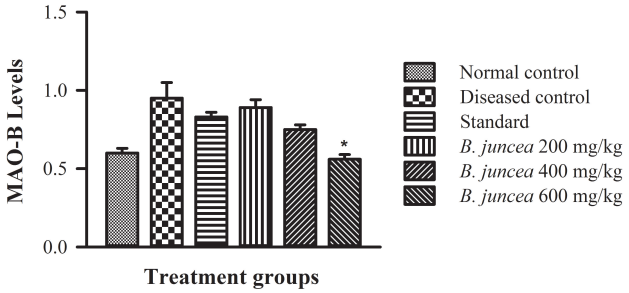

Fig. 5. Effect of *B. juncea* extract on MAO-B levels in the brain of rats.
*$p < 0.05$ compared to the disease control.

ited better recovery from haloperidol-induced brain damage as shown in Fig. 6.

3.4 Molecular docking analysis

Molecular Operating Environment (MOE) software package 2016.10 was used for molecular docking of AchE protein with selected 12 phytochemicals. Molecular docking analysis explains the functional residues involved in the inhibitory activity of AChE protein to design a potential drug against PD by using the dataset of 12 phytochemicals (Table 3).

Molecular docking interpretations show that the binding energies of best-bounded confirmation of the selected 12 phytochemicals were in the range of –7.8793 to –4.4390 Kcal/mol. As the molecule that has presented the lowest binding energy was considered the most significant AChE inhibitor. So that there are four ligands (sinapic acid, rutin, ferulic acid, and caffeic acid), that were considered to be the best AChE inhibitors based on their best-bounded confirmation, lowest binding affinities, and excellent binding interactions within the catalytic pocket of enzyme AChE (PDB ID: 4EY7) (Fig. 7). Other 7 phytochemicals have also presented significant interactions in terms of Vader Waals or hydrophobic interactions, hydrogen bonds, Pi-lone pair, Pi-Pi T-shaped, and Pi-alkyl interactions, but their binding energies were not up to the significant threshold value (Table 4).

For the entry into AChE, target protein's through the active binding site, there is a narrow cleft linked with the pattern of aromatic amino acid residues, hence allow the substrate to enter into the catalytic triad of HIS, SER, and GLU amino acid residues. It is known as the hydrophobic amino acid residues are linked with the aromatic amino acids supervision that revealed the highest degree of flexibility and permits the ligands of significant size. Though, the opening and closing posture of the active site is associated with a fluctuating cleft e.g. ligand atoms interacting with TYR337 residue [28]. The conformational investigation exposed that sinapic acid, ferulic acid, and caffeic acid, penetrated the active site cleft, and interrupted the aromatic amino acids, and inhibit the substrate-binding (Fig. 7). Moreover, these ligands accept the challenge of blocking the fluctuating cleft and overturned near the catalytic triad to inhibit the target protein activity [29].

Sinapic acid has achieved the lowest binding energy (–7.8793 Kcal/mol) of the best-bounded conformation and presented the highest potential towards inhibition of AChE protein expression. Functional residues of the active site such as THR83, ASN87, GLY121, SER125, TYR133, GLU202, ALA204, TRP236, TYR341, GLY448, and ILE451 are responsible for the weak Vader Waals and hydrophobic interaction network, while seven hydrogen bonds were generated by ASP74, GLY120, GLY122, SER203, TYR337, and TYR124 residues. TRP86 residue is applicable for Pi-lone pair association, Pi-Pi stacking with T-shaped geometry has been visualized by the interaction of TYR337 residue. PHE295, PHE297, PHE338, and HIS447 residues were found to establish the significant influence of Pi-alkylation. Hence, the atoms of sinapic acid are showing considerable interactions with the target protein residues in Fig. 7a,b.

Rutin has also presented significant binding energy (–7.0091 Kcal/mol) of the best-bounded conformation as a result of docking investigation with AChE protein, and it has been very good docked results. THR75, VAL282, ASN283, HIS284, TRP286, HIS287, GLN291, and SER293 residues are responsible for hydrophobic interactions and six hydrogen bonds were generated by TYR72, ASP74, LEU76, GLU292, TYR341, and GLY342 residues within the catalytic cleft of the enzyme AChE, most of the ligand surface was exposed towards the solvent shown by the blue blobs in Fig. 7c,d.

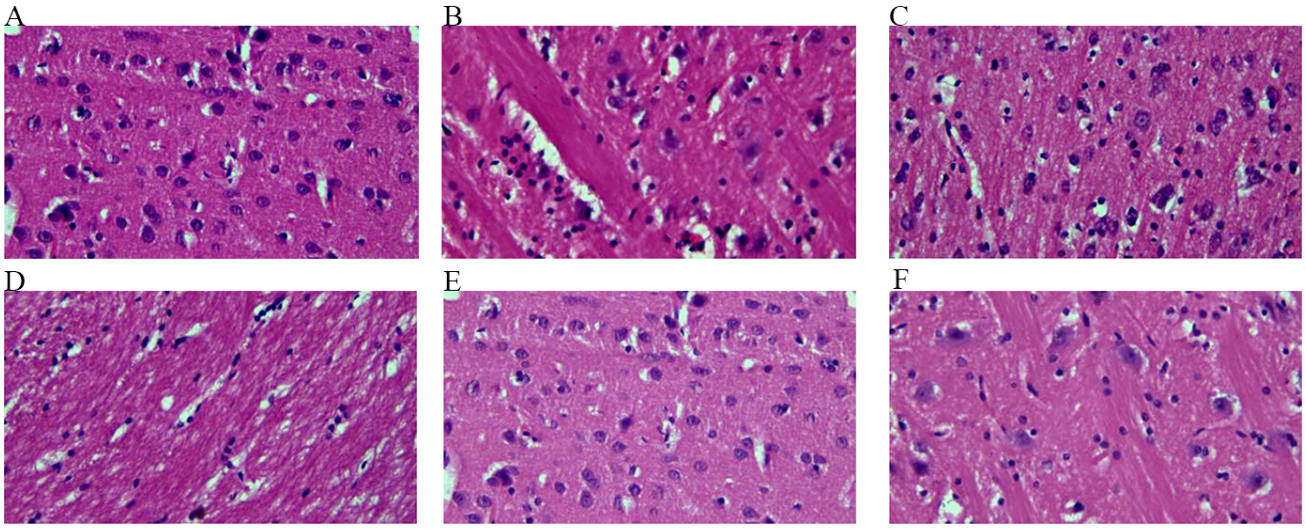

Fig. 6. Effect of *B. juncea* extracts on histopathology of brain tissue in haloperidol-induced parkinsonism in rats (at 40×). (A) normal control. (B) disease control. (C) standard. (D) *B. juncea* 200 mg/kg. (E) *B. juncea* 400 mg/kg. (F) *B. juncea* 600 mg/kg.

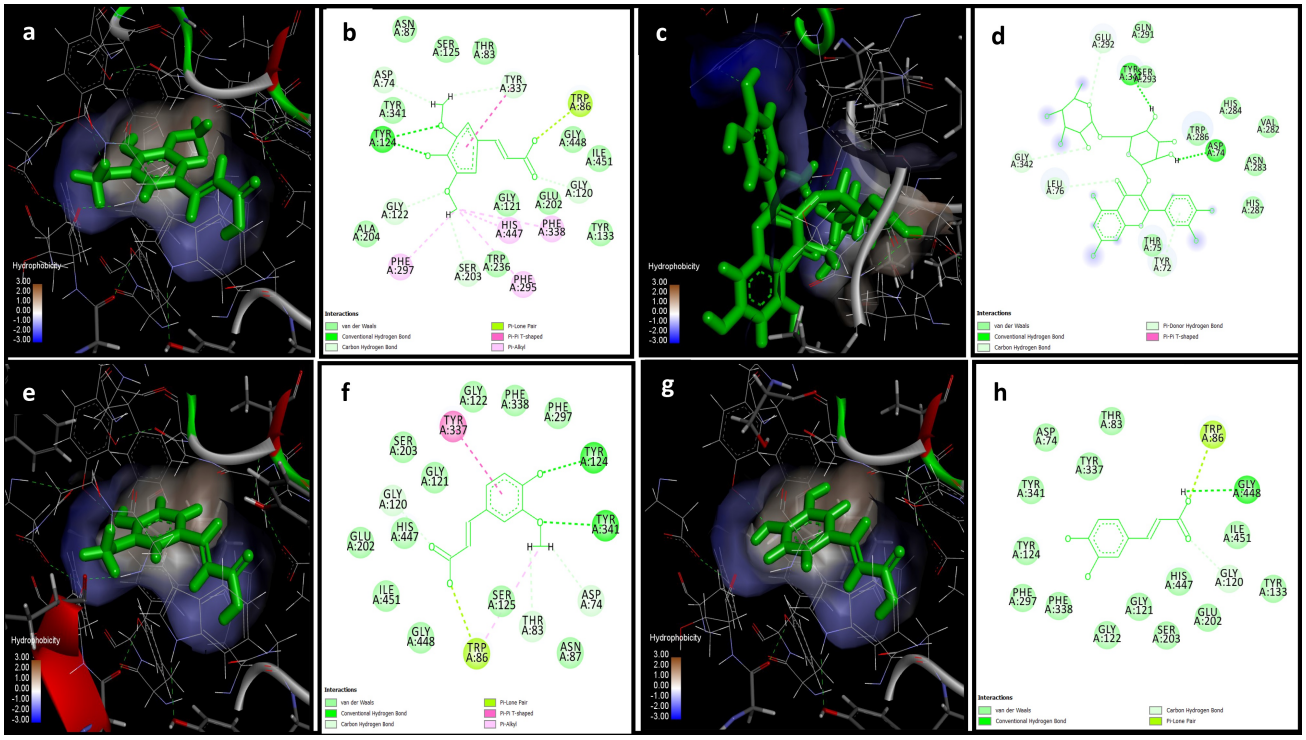

Fig. 7. Three-dimensional representation of the hydrophobic molecular surface of the Acetylcholine-esterase (AchE) protein (PDB ID: 4EY7) with respective docked phytochemicals; Sinapic acid. (a) Rutin, (c), Ferulic acid (e), and Caffeic acid (g) within an active binding site. While two-dimensional interaction plot presents significant binding interactions of the four top-scored bound ligands; Sinapic acid (b), Rutin (d), Ferulic acid (f), and Caffeic acid (h) within a distance range of 4Å. Interactions were shown by dotted lines and residues were classified by different colors, as indicated in the legend below the interaction plot.

Ferulic acid exhibited the strongest binding affinity in terms of the lowest energy value (–7.0991 Kcal/mol), and also depicted the largest network of significant binding interactions within the vicinity of the active binding site of AChE protein. ASN87, GLY120, GLY121, GLY122, SER125, GLU202, SER203, PHE297, PHE338, HIS447, GLY448, and ILE451 are involved in hydrophobic interactions. ASP74, THR83, TYR124, TYR341, and GLY120, residues were responsible for the generation of five hydrogen bonds. TRP86 formed the Pi-lone pair. TYR337 residue was associated with Pi-Pi T-shaped bonding and TRP86 residue was showing Pi-alkylation. Fig. 7e,f shows

Table 3. Molecular docking results of AChE protein with selected phytochemicals.

PubChem CID	Compound names	Binding energies (Kcal/mol)	Functional residues	Binding interactions
1057	Pyrogallol	–4.5346	TYR83, TRP86, GLY120, GLY121, GLY122, TYR124, GLU202, SER203, PHE295, PHE297, TYR337, PHE338, TYR341, HIS447, GLY448	Vader Waals, Hydrogen bonds, Pi-Pi T shaped
370	Gallic acid	–5.4270	THR83, TRP86, GLY120, GLY121, GLY122, TYR124, GLU202, SER203, ALA204, PHE297, TYR337, PHE338, TYR341, HIS447, GLY448, ILE451	Vader Waals, Hydrogen bonds
289	Catechol	–4.4390	THR83, TRP86, GLY120, GLY121, GLY122, TYR124, GLU202, SER203, PHE295, PHE297, TYR337, TYR341, HIS447, GLY448	Vader Waals, Hydrogen bonds, Pi-Pi T shaped
73160	Catechin	–5.5765	TYR72, ASP74, LEU76, TYR124, TRP286, VAL294, PHE295, ARG296, PHE297, PHE338, TYR341	Vader Waals, Hydrogen bonds, Pi-Pi T shaped, Pi-Alkyl
135	Hydroxybenzoic acid	–5.5133	ASP74, THR83, TRP86, ASN87, GLY120, GLY122, TYR124, SER125, SER203, PHE297, TYR337, PHE338, TYR341, HIS447	Vader Waals, Hydrogen bonds, Pi-Pi T-shaped
1794427	Chlorogenic acid	–5.8612	TYR72, ASP74, THR75, LEU76, GLN250, TRP286, HIS287, LEU289, GLN291, GLU292, SER293, VAL294, TYR341	Vader Waals, Hydrogen bonds
689043	Caffeic acid	–6.3780	ASP74, THR83, TRP86, GLY120, GLY121, GLY122, TYR124, TYR133, GLU202, PHE297, TYR337, PHE338, TYR341, HIS447, GLY448, ILE451	Vader Waals, Hydrogen bonds, Pi-Lone Pair
637775	Sinapic acid	–7.8793	ASP74, THR83, TRP86, ASN87, GLY120, GLY121, GLY122, TYR124, SER125, TYR133, GLU202, SER203, ALA204, TRP236, PHE295, PHE297, TYR337, PHE338, TYR341, HIS447, GLY448, ILE451	Vader Waals, Pi-Pi T shaped, Pi-Lone Pair, Hydrogen bonds, and Pi-Alkyl
637542	Coumaric acid	–5.8149	ASP74, TRP86, GLY120, GLY121, GLY122, TYR124, TYR133, GLU202, SER203, PHE297, TYR337, PHE338, TYR341, HIS447, GLY448	Vader Waals, Hydrogen bonds, Pi-Lone Pair, Pi-Pi T-shaped
445858	Ferulic acid	–7.0991	ASP74, THR83, TRP86, ASN87, GLY120, GLY121, GLY122, TYR124, SER125, GLU202, SER203, PHE297, TYR337, PHE338, TYR341, HIS447, GLY448, ILE451	Vader Waals, Pi-Pi T-shaped, Pi-Lone Pair, Hydrogen bonds, Pi-Alkyl
5280805	Rutin	–7.0091	TYR72, ASP74, THR75, LEU76, VAL282, ASN283, HIS284, TRP286, HIS287, GLN291, GLU292, SER293, TYR341, GLY342	Vader Waals, Hydrogen bonds, Pi-Pi T-shaped
6911854	Sinigrin	–6.2601	TYR72, THR75, LEU76, TYR124, LEU285, TRP286, HIS287, GLY289, GLN291, GLU292, SER293, VAL294, PHE295, ARG296, PHE297, TYR341, GLY342	Vader Waals, Hydrogen bonds, Pi-Sulfur, Pi-Alkyl

the most of the interacting catalytic surface of the selected enzyme AChE is hydrophobic, and atoms of the ferulic acids make significant binding interactions with the residue present in the native binding pocket of the AChE target protein.

Caffeic acid has presented the -6.3780 Kcal/mol binding energy within the active site of target protein, most of the interacting residues such as ASP74, THR83, GLY120, GLY121, GLY122, TYR124, TYR133, GLU202, PHE297, TYR337, PHE338, TYR341, HIS447, and ILE451are involved in the hydrophobic interaction network, while GLY448 and GLY120 have generated two hydrogen bonds with the atoms of caffeic acid. Pi-lone pair association was observed between the ligand atom and TRP86 residue of target protein shown in Fig. 7g,h.

The active content of *Brassica juncea*, sinigrin has also been studied to check its binding potential with acetylcholine-esterase (AchE) protein (PDB ID: 4EY7) and bounded at the best conformation at -6.2601Kcal/mol and interacted with TYR72, THR75, LEU76, TYR124, LEU285, TRP286, HIS287, GLY289, GLN291, GLU292, SER293, VAL294, PHE295, ARG296, PHE297, TYR341,

and GLY342 functional residues of the active site of the target protein. TRP286 has generated Pi-sulfur contact, TYR124, PHE297, and TYR341 have generated Pi-alkyl contacts, TYR72, GLU292, and GLY342 have generated hydrogen bonds, and TYR75, LEU76, HIS287, LEU289, GLN291, Val294, PHE295, and ARG296 residues are involved in the Vander Waals interactions with atoms of sinigrin (Table 3).

The docking results of sinapic acid, ferulic acid, and caffeic acid are excellent in terms of binding interactions with functional residues and their docked complex binding energies are above 7 Kcal/mol and shown the strongest efficacy towards the AChE target protein among the selected 12 phytochemicals. Moreover, the other contents of Brassica juncea extracts, caffeic acid, and sinigrin has exhibited binding energies of less than 7 Kcal/mol which is less than the good threshold values, and shown moderate protein-ligand interaction results and energy values in the range of 6 to 7 Kcal/mol. The other six phytochemicals; Pyrogallol, gallic acid, catechol, catechin, hydroxybenzoic acid, chlorogenic acid, coumaric acid, and rutin have presented binding energies less than 6 Kcal/mol that is less than the threshold values. It means the docking results show less potential of these six compounds towards inhibition of AChE target protein.

3.5 Pharmacokinetics and toxicity risk assessment

Calculation of *in silico* pharmacokinetic parameters is significant to narrow down the large dataset to highly significant drugs with the minimum risk of rejection in the early drug development procedures [29]. Four best-scored phytochemicals were subjected for the estimation of *in silico* pharmacokinetic properties by Swiss ADME and toxicity estimations by Osiris molecular property explorer. Hence, three phytochemicals, sinapic acid, ferulic acid, and caffeic acid showed the maximum results in the acceptable range shown in Tables 4 and 5.

The drug or compound we selected should be metabolized by the body or not, it is required to be understood because the only pharmacokinetics properties won't be enough to understand the membrane permeability of selected phytochemicals. After all, the high logP and molecular weights of the compounds from natural sources could not accept the drug-likeness parameters, although in several studies *in silico* drug-like calculations have been performed [30] while in this study three phytochemicals have shown that they have accepted the rules of drug-likeness, and only one compound rutin has violated the rule due to its large chemical compound size.

Additionally, cytochromes P450 were calculated to support the pharmacokinetics of the selected phytochemicals, it is reported that the essential isoforms, e.g., CYP1A2, CYP2C19, CYP2C9, CYP2D6, and CYP3A4 are important for drugs activity within the body. The mechanism of isoforms of the cytochrome P450 superfamily is becoming a challenge for the natural chemicals concerning the metabolism and excretion of drugs through the liver [31]. Chemicals that could inhibit the cytochromes P450 assist the interactions of selected natural compounds and are attributable to drug administration that may not be able to encompass the metabolism-related activity and accumulate as toxic substantials inside the body.

Lipophilicity (LogP) values are also calculated for the four putative phytochemicals because it is important to explain the bioavailability of the drug, some minor violations were observed in three selected phytochemicals other than rutin, these drug-like parameters assist the oral administration of chemicals, such as poor lipophilic drugs corresponding to poor gastrointestinal (GI) absorption and owns the lowest BBB permeability, so it's critical to understand the protein-ligand interactions intricated in the disease of the central nervous system [32]. The water solubility (LogS) of the phytochemical was calculated to describe the absorption and distribution, all four chemicals have presented very good solubility and all these properties were explained well in Tables 4 and 5.

The undesired or unnecessary structural issues known as Pan assay interference compounds (PAINS) and Brenk alerts were also studied in the four selected phytochemicals, it is thought to be eliminated before moving towards the early drug development procedures [28]. All four phytochemicals have displayed PAINS and Brenk alerts, which could be a preliminary hypothesis and could be helpful for the improvement of structural issues. Osiris molecular property explorer demonstrated that four phytochemicals results are positive, there are no harmful effects on four major grounds of tumorigenic, mutagenic, irritant, and reproductive properties, Moreover, drug-likeness and drug scores are important to understand the ADMET profile of a chemical, that is also very good and acceptable result are shown in Table 5 and Fig. 8. Hence, it is demonstrated that the ADMET profile of the selected phytochemicals along with the protein-ligand interaction results is most acceptable, so our proposed chemical compounds could be potential inhibitors of the AChE protein target and treat the PD well [31].

4. Discussion

Parkinson's disease (PD) is a chronic brain disorder. It is slowly progressive and characterized by tremors, rigidity, stiffness, and difficulty in walking [6]. Non-motor symptoms are usually associated with cognitive decline and behavioral abnormalities and worsen in the advanced stages of this disease [33]. The motor symptoms of PD are mainly induced by dopaminergic neuronal apoptosis in substantia

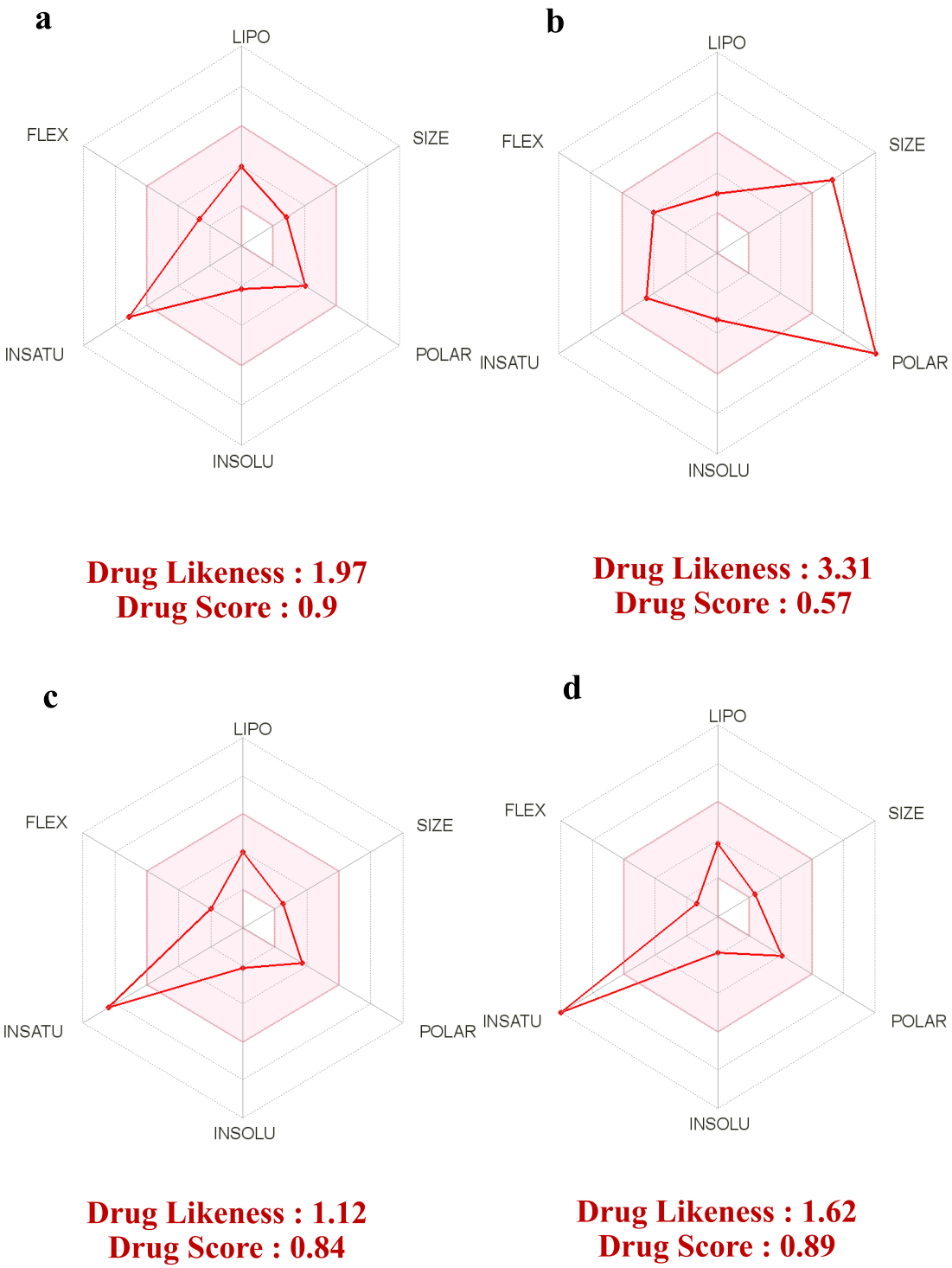

Fig. 8. Schematic representation of ADMET profile of top score four phytochemicals; sinapic acid (a), rutin (b), ferulic acid (c) and caffeic acid (d). The pink-colored area depicted the acceptable pharmacokinetic parameters. All four extracted chemical compounds have demonstrated very good results, fulfilling the drug-likeness rules except rutin because of its large size it has a high molecular weight, moreover, the drug scores are in the acceptable range, while sinapic acid has presented the best result.

Table 4. Summary of drug-likeness and *In silico* pharmacokinetic properties of the extracted best phytochemicals by SwissADME server.

Chemical parameters		Sinapic acid	Rutin	Ferulic acid	Caffeic acid
	SMILES Notation	COC1=CC(=CC(=C1O)OC)C=CC(=O)O	CC1C(C(C(C(O1)OCC2C(C(C(O2)OC3=C(OC4=CC(=CC(=C4C3=O)O)O)C5=CC(=C(C=C5)O)O)O)O)O)O)O	COC1=C(C=CC(=C1)C=CC(=O)O)O	C1=CC(=C(C=C1C=CC(=O)O)O)O
	Formula	C11H12O5	C27H30O16	C10H10O4	C9H8)4
	Molecular weight (MW) (g/mol)	224.21	610.52	194.18	180.16
	Heavy atoms	16	43	14	13
	Aromatic Heavy atoms	6	16	6	6
	Fraction Csp3	0.18	0.44	0.10	0.00
	Rotatable bonds	4	6	3	2
	Hydrogen bond acceptors (HBA)	5	16	4	4
	Hydrogen bond donors (HBD) Molar	2	10	2	3
	Refractivity (MR)	58.12	141.38	51.63	47.16
	Total polar surface area (TPSA) (Å)	75.99	269.43	66.76	77.76
Lipophilicity					
	LogPo/w (iLOGP)	1.63	2.43	1.62	0.97
	LogPo/w (XLOGP3)	1.46	–0.33	1.51	1.15
	LogPo/w (WLOGP)	1.40	–1.69	1.39	1.09
	LpgPo/w(MLOGP)	0.73	–3.89	1.00	0.70
	LogPo/w (SILICOS-IT)	1.33	–2.11	1.26	0.75
	Consensus Log Po/w	1.31	–1.12	1.36	0.93
Water solubility					
	LogS (ESOL)	–2.16	–3.30	–2.11	–1.89
	Solubility (mg/mL)	1.54	3.08	1.49	2.32
	Class	Soluble	Soluble	Soluble	Most soluble
	LogS (Ali)	–2.66	–4.87	–2.52	–2.38
	Solubility (mg/mL)	4.88	8.30	5.86	7.55
	Clas	Soluble	Moderately Soluble	Soluble	Soluble
	LogS (SILICOS-IT)	–1.55	–0.29	–1.42	–0.71
	Solubility (mg/mL)	6.33	3.15	7.43	3.51
	Class	Soluble	Soluble	Soluble	Soluble
Pharmacokinetics					
	GI absorption	High	Low	High	High
	BBB permeant	No	No	Yes	No
	P-gp substrate	No	Yes	No	No
	CYP1A2 inhibitor	No	No	Yes	No
	CYP2C19 inhibitor	No	No	No	No
	CYP2C9 inhibitor	No	No	No	No
	CYP2D6 inhibitor	No	No	Yes	No
	CYP3A4 inhibitor	No	No	Yes	No
	Log Kp (skin permeation) (cm/s)	–6.63	–10.26	–6.41	–6.58

Table 4. Continued.

Chemical parameters		Sinapic acid	Rutin	Ferulic acid	Caffeic acid
Drug-likeness					
	Lipinski	No violations	3 violations MW >500, HBA >10, HBD >5	No violations	No violations
	Ghos	No violations	4 violations MW >500, WLOGP <–0.4, MR >130, Num of atoms >70	No violations	No violations
	Veber	No violation	1 violation TPSA >140	No violations	No violations
	Egan	No violation	1 violation TPSA >131.6	No violations	No violations
	Muegge	No violations	4 violations MW >600, TPSA >150, HBA >10, HBD >5	No violations	1 violations MW <200
	Bioavailability Score	0.56	0.17	0.85	0.58
Medicinal chemistry-related properties					
	PAINS	No alert	1 alert Catechol_A	No alert	1 alert Catechol_A
	Brenk	1 alert Michael_acceptor_1	1 alert Catechol	1 alert Michael_acceptor_1	2 alert Catechol, Michael_acceptor_1
	Lead likeness	1 violations MW <250	1 violation MW <250	1 violations MW <250	1 violations MW <250
	Synthetic accessibility	2.17	6.52	1.93	1.81

Table 5. ADMET profile of best four phytochemicals assessed by Osiris molecular property explorer.

Chemical descriptors	Sinapic acid	Rutin	Ferulic acid	Caffeic acid
Irritant	No effects	No effects	No effects	No effects
Mutagenic	No effects	No effects	No effects	No effects
Tumorigenic	No effects	No effects	No effects	No effects
Reproductive properties	No effects	No effects	No effects	No effects
cLogP	0.99	–1.26	1.06	0.78
Solubility	–1.74	–2.4	–1.72	–1.41
MW	224	610	194	180
TPSA	75.99	265.5	66.76	77.76
Drug-likeness	1.97	3.31	1.12	1.62
Drug score	0.9	0.57	0.84	0.89

nigra pars compacta and brought about dopamine deficiency [34]. Until now, no cure for this disease is available. Although, the conventional treatment with levodopa, monoamine oxidase inhibitors, and dopamine agonists are effective only in the early stages. These therapeutic agents are ineffective and associated with severe side effects in advanced stages such as involuntary muscular movements [35]. Oxidative stress, mitochondrial dysfunction, neuronal apoptosis, neuronal excitotoxicity, and accumulation of misfolded proteins like alpha-synuclein are major pathological hallmarks. Due to the existence of a higher amount of dopamine and its metabolites, the substantia nigra of the middle brain is more vulnerable to oxidative stress [36].

Most of the medicinal plants enriched with alkaloids, flavonoids, and polyphenols have been reported with neuroprotective and antioxidant potential against neurodegenerative disorders [37]. In the current study, HPLC analysis of *B. juncea* revealed the existence of a favorable amount of polyphenolic antioxidant compounds. Catechol and hydroxyl benzoic acid existed in higher concentrations (mg/g of plant extract) compared to other compounds in ethanol extract of *B. juncea.* Congruent to previous study catechol polyphenolic compounds and lipids compounds are associated with neuroprotective, anti-inflammatory, and antioxidant potential in oxidative stress-induced neurotoxicity in rat brain and modulated dopamine neurotransmission [38, 39]. Hydroxy benzoic acid in *B. juncea* is associated with antioxidant and neuroprotective effects in the PD model similar to reported literature in which this compound remarkably mitigated the pathological hallmarks of neurodegeneration through modulation of antioxidant and anti-neuro-inflammatory signaling pathways [40, 41]. A favorable amount of antioxidant rutin is detected in ethanol extract of *B. juncea*, which is associated with therapeutic potential to reverse the neurodegeneration via modulation of brain-derived neurotrophic factor, nerve growth factor, and through inhibition of neuronal apoptosis in rat brain in previous studies [42]. In the repeated cerebral ischemic rat model of impaired spatial memory, rutin ameliorated neuronal death and spatial memory impairment [42, 43]. Pyrogallol [44, 45], gallic acid [46–48], catechin [49], chlorogenic acid [50], caffeic acid [51], sinapic acid [52], coumaric acid [53], and ferulic acid [54] found in ethanol extract of *B. juncea* are responsible for neuroprotective effect against haloperidol-induced neurotoxicity in corroboration to previously reported literature through modulation of Nrf2/OH-1 -1 pathway and other antioxidant signaling pathways, neuronal cell death, and mitochondrial dysfunctions. In this study detection of antioxidant compounds through Hplc analysis is supported by DPPH scavenging assay [55]. *B. juncea* as a source of antioxidants exhibited free radical scavenging/inhibiting potential, therefore could be effective in the treatment of numerous oxidative stress associated with human ailments [37].

The neuroprotective role of *B. juncea* was evaluated in haloperidol-induced PD in the rat. Haloperidol-induced catalepsy is widely accepted in an animal model of PD through the non-selective blockade of D_2 receptors leading to dopamine exhaustion at nerve endings. So that haloperidol (1mg/kg) induced catalepsy was remarkably recovered by *B. juncea* ethanol extract in a dose-dependent manner demonstrating the neuroprotective role of plant extract through modulation of dopamine neurotransmission [56].

Hang test revealed that *B. juncea* extracts improved neuromuscular coordination and muscular strength impaired by haloperidol injection and showed a correlation with the findings of our previous research published in 2020 [36]. While the results concluded from this study have presented a similar horizontal bar test as mentioned in our other published research work [57] indicated that administration of *B. juncea* extract mitigated the haloperidol-induced motor dysfunctions and recovered the locomotion abnormalities.

Haloperidol-induced reversible blockade of D_2 receptors results in the generation of free radicals. Free radicals perpetuated mitochondrial dysfunctions and neuronal death. Oxidative stress was measured in this study through the estimation of catalase activity, superoxide dismutase, malondialdehyde, and reduced glutathione level in brain homogenates [58].

Haloperidol-induced neurotoxicity through the production of free radicals and hydrogen peroxide due to its inhibitory potential on mitochondrial complex I and IV in the electron transport chain. These free radicals induced lipid peroxidation, protein denaturation in brain tissues of PD patients [59]. Lipid peroxidation was assessed through estimation of the thiobarbituric acid level in brain homogenate as a sensitive biomarker of oxidative stress [60]. Unsaturated fatty acids and arachidonic acids are vulnerable to radical attack and produce lipid peroxyl radicals, perpetuating further initiation of free radicals chain reaction and attack on the double bond of unsaturated fatty acids [61]. Lipid peroxidation induced impaired structural and functional integrity of biological membrane leading to deactivation of membrane-bound enzymes [62]. The raised level of lipid peroxidation and products are found in substantia nigra PD brain tissues. Lipid peroxidation marker, Malnodialdehyde level was increased in brain tissues after haloperidol treatment compared to control similar to previous findings. *B. juncea* extract ameliorated the raised level of Malnodialdehyde and decreased lipid peroxidation due to its antioxidant potential. Hydrogen peroxide produced in brain tissues is neutralized by catalase into the water and molecular oxygen and inhibited the accumulation of precursors for the biosynthesis of free radicals. The decreased level of catalase is reported in PD brain tissues congruent to the current study. *B. juncea* extract recovered the reduced level of catalases in brain tissues similar to previous findings [35]. The dismutation of superoxide reaction is cat-

alyzed by superoxide dismutase as a first-line antioxidant defence system in most of the cells. Haloperidol decreased the level of superoxide dismutase in this study parallel to our previous findings. However, *B. juncea* extracts improved the decreased level of superoxide dismutase. The dopaminergic neuronal loss resulted due to decreased level of reduced glutathione level in the PD brain [57].

Reduced levels of reduced glutathione impaired the neuron to detoxify hydrogen peroxide and raised oxidative stress. It was evident from the present study that haloperidol declined the level of reduced glutathione similarly as reported earlier [57]. Though, *B. juncea* extract decreased the oxidative stress by retrieving the level of reduced glutathione in treatment groups. Therefore, it is evident from biochemical analysis that *B. juncea* extract has antioxidant potential, and findings are also supported by histopathological analysis. In the current study histopathological findings showed a protective effect of *B. juncea* extract on neuronal necrosis, neuronal density, intracellular spaces, and neutrophil infiltration in the striatum region of the brain [58]. Therefore, it is concluded from the present study that *B. juncea* extract has neuroprotective potential against neurotoxicity caused by haloperidol through modulation of behavioral and biochemical parameters and will be considered as a lead compound in the future neurotherapeutic to treat cureless neurodegeneration.

All 12 phytochemicals extracted from *B. Juncea* have also presented significant interactions in terms of Vader Waals or hydrophobic interactions, Pi-alkyl, hydrogen bonds, Pi-lone pair, Pi-Pi T-shaped interactions within the native active binding site of the target protein (Table 4). Computational analysis of the proposed results of the extracted compounds has explained that four phytochemicals have presented very good results in terms of protein-ligand binding interactions as well as ADMET profile estimations (Figs. 7 and 8). Following isolated selected compounds evaluated in the integrated experimental and computational study have shown antioxidant potential and it is also highlighted in previous literature, hence providing support to our concluded results [17, 63, 64]. Sinapic acid, ferulic acid, and caffeic acid are excellent AChE inhibitors with binding energies above 7 Kcal/mol. While caffeic acid and sinigrin have exhibited moderate AChE inhibitory potential with binding energies in the range of 6 to 7 Kcal/mol. The other six phytochemicals; Pyrogallol, gallic acid, catechol, catechin, hydroxybenzoic acid, chlorogenic acid, coumaric acid, and rutin are weak AChE inhibitors. Tables 4 and 5 enlisted ADMET properties of the four putative phytochemicals, and seems are very much acceptable, only rutin have presented more violations because of its large chemical size, moreover, Fig. 8 shows that all four phytochemicals drug-likeness and drug scores are in the acceptable range, and sinapic acid is showing the remarkable ADMET properties as well as drug-interactions within the active binding site of AChE target protein. Sinapic acid has been evaluated for brain diseases previously and has shown remarkable results [65, 66]. In vitro and *in vivo* studies also highlighted the efficacy of the natural components of the *B. juncea* leaves for PD and neuroprotective disorders.

5. Materials and methods

5.1 Plant collection and identification

The *B. juncea* leaves were collected in the winter season from Toba Tek Singh district, Pakistan. The herbarium of *B. juncea* plant was prepared and identified from the Department of Botany, Government College University Faisalabad by Taxonomist Dr. Qasim Ali under authentication number Z245-BOT-19.

5.2 Physiochemical analysis and quantitative phytochemical analysis

The physicochemical analysis of *B. juncea* leaves powder including loss on drying, total ash, acid-insoluble, water-insoluble and sulfated ash contents, alcohol and water-soluble contents were performed by following United States Pharmacopoeia-National Formulary (2003) methods [67]. Das *et al*. (2018) [68] method was adopted for the quantification of alkaloids and Saleem *et al*. (2014) [69] methods were followed for the flavonoids and phenolic contents determination.

5.2.1 Physicochemical analysis

5.2.1.1 Loss on drying

Two-gram of plant powdered was dried in the oven for 30 minutes at 105 °C by putting it in the tarred china dish. After cooling, the dried plant was weighed. Moisture content was calculated as a loss on drying by dividing the dried weight with actual powdered plant weight.

5.2.1.2 Total ash

Two gram of plant powder was incinerated in the electric furnace at 675 ± 25°C until it got free from carbon. This carbon-free ash was cooled in the desiccator and weighed. Total ash content was calculated by dividing the ash weight with the initial powdered weight.

5.2.1.3 Water-insoluble ash

Total ash obtained in the previous ash test was boiled with 25 mL of distilled water for five minutes and then filtered through ashless filter paper. The filtrate contained the soluble material of the plant and residue on the filter paper was an insoluble matter that was washed with warm distilled water to extract any soluble material in the residue. Then filter paper was dried and ignited in the china dish (that was pre-tarred) till the carbon-free ash was obtained. After cooling this ash, it was weighed and water-insoluble ash was calculated by dividing this ash weight with the initial total ash weight.

5.2.1.4 Acid-insoluble ash

Total ash obtained in the previous ash test was boiled with 25 mL of HCl for five minutes and then filtered through ashless filter paper. The filtrate contained the soluble material of the plant and residue on the filter paper was an insoluble matter that was washed with warm distilled water to extract any soluble material in the residue. Then filter paper was dried and ignited in the china dish (that was pretarred) till the carbon-free ash was obtained. After cooling this ash, it was weighed and acid-insoluble ash was calculated by dividing this ash weight with the initial total ash weight.

5.2.1.5 Sulfated ash

Two grams of plant powder were put in the china dish and sulphuric acid was added to it to make a paste-like material. This china dish was put on the burner, white fumes started to originate and ignition was done till the white fumes ended to arise. Then it was cooled and ash content was weighed.

5.2.1.6 Alcohol and water-soluble extractives

In the tarred flask, 5 grams of powdered plant material was placed and macerated with 100 mL of 95% ethanol (in case of alcohol-soluble extractive) and 100 mL distilled water in case of water-soluble extractive for 24 hours. Then extract was filtered and in the china dish, 25 mL of filtrate was evaporated till residue remained at the bottom. This residue was further dried in the oven at 105 ^{o}C and weighed. The percentage of the extractives was calculated regarding the weight of the powdered material used in the test.

5.2.2 Phytochemical quantification

5.2.2.1 Quantification of alkaloid content

One gram extract was mixed with dimethyl sulfoxide in the test tube and 1 mL of 2 N HCl was added to this test tube. The solution was filtered using Whatman no. 1 filter paper and 5 mL bromocresol green solution along with 5 mL phosphate buffer was added to it. The mixture was shaken thoroughly. After that, trichloromethane was added at different quantities as 1-, 2-, 3-, and 4 mL. Then the mixture was added to a 10 mL volumetric flask and dilution was made with trichloroacetic acid. Standard atropine solution at different concentrations 10-, 20-, 30-, 40-, 50- and 60 μg/ml were made similarly to that of extract (test sample). The absorbance of a test sample and reference sample was measured by an ultraviolet spectrophotometer at 470 nanometers. A blank sample was used for error correction. The presence of total alkaloids in the extract was measured as milligrams of atropine equivalent (AEq/g) of extract.

5.2.2.2 Quantification of phenolic content

The phenolic content of the extract was calculated by using Folin-Ciocalten's reagent method. In this method, 1 mL of sample and 1 mL of standard solution were mixed in a test tube then phenolic reagent 0.2 mL was added to it and mixed thoroughly. After 4 minutes, 1 mL of a sodium carbonate solution was added and stored in the darkness. Various concentrations (10-, 20-, 30-, 40-, 50- and 60 μg/ml) of the reference sample were prepared similarly to that of the test sample (extract) to make a standard curve. The absorbance of the test sample and reference sample was recorded at 750 nm. The percentage of total phenolic content was calculated using the following equation:

$$T = \frac{C * V}{M}$$

Here, T = total phenolic content (mg/g), C = gallic acid equivalent (μg/mL), V = volume of extract (mL), M = weight of the extract (g).

5.2.2.3 Quantification of flavonoid content

The total flavonoid content of the extract was calculated by using the $AlCl_3$ colorimetric method. Extract 0.3 mL was added to the test tube. Then 3.4 mL of methanol 30%, 0.15 mL of 0.5 M sodium nitrite, and 0.15 mL of aluminum trichloride hexahydrate (0.3 M) were added to the test tube having a sample in it and after few minutes, the 1 mL solution of sodium hydroxide (1 M) was added. Quercetin was used as a reference sample. Reference solution was made similarly to that of sample extract. The standard curve was constructed by drawing the graph between various concentrations (10-, 20-, 30-, 40-, 50- and 60 μg/mL) of quercetin vs respective absorbance. Blank was prepared identically to that of the sample but it was without extract/reference sample. The mixture was shaken well and absorbance was measured against the blank at 506 nm. Total flavonoid content was determined as mg of quercetin equivalents/g of ethanol extract.

5.3 High-performance liquid chromatography (HPLC) analysis

The methanolic Plant extract was filtered through a 0.2 μm membrane filter (Millex-HV) and injected into HPLC. The HPLC system (Shimadzu LC-20AT) was used. Mobile phase composed of (A) 0.1% acetic acid and (B) methanol and the composition gradient was: 25% (B) for 10 min; 40% (B) for 15 min; then 50%, 60%, 80% and 100% (B) for every 10 min. The flow rate was 0.8 mL min^{-1}. Phenolic moieties were acknowledged with the spectra of standard compounds at 280 nm [70].

5.4 Extract preparation by microwave-assisted extraction method

B. juncea leaves were washed thoroughly with tap water and the leaves were dried in a hot air oven at 40 °C temperature. Then, the leaves were crumbled to fine powder by utilizing an electronic blender. The powder was passed over a sieve and deposited in an airtight container. The 100 g powder of *B. juncea* was weighed and taken in each of 3 beakers that contain 750 mL ethanol each. All three beakers were placed in a microwave oven already adjusted at 9000 watt, and then the oven heated up for 2 min, stopped the oven, and opened it for 30 sec. This specific method was repeated 5 times. In the end, the supernatant was filtered through filter paper. In the 2nd cycle again 500 mL ethanol was added in each beaker containing residue. Again all the beakers were placed in a microwave oven. The oven was heated up for 2 minutes and then stopped for 30 seconds. The same method was repeated 5 times. The supernatant solution was filtered through filter paper. In the 3rd cycle again 500 mL ethanol was added to each beaker and repeated the same method 5 time. Filtrates were pooled in the same reservoir. Excess solvent was removed from the filtrate/extract using a rotary evaporator at 40 °C and semisolid ethanolic leaves extract (ELE) was obtained. Lipids were removed by washing the extract with n-hexane. It was stored in a refrigerator at 4 °C till further use.

5.5 Determination of antioxidant potential

The *in vitro* antioxidant properties of *B. juncea* ethanol extract were determined by 2,2-diphenyl-1-picryl-hydrazyl (DPPH) free radical scavenging assay by the earlier procedure [68]. The extract solution at different concentrations (25-, 50-, 100-, 150- and 200 μg/mL) was prepared in methanol by two-fold dilution method while ascorbic acid solution (1-100 μg/mL) that was prepared in methanol, used as standard. For the test, 500 μL DPPH solution (0.1 mM) was added in 250 μL of extract solution and 250 μL of methanol. The solution was allowed to stand at 25 °C for half an hour in a dark place and absorbance was measured at 517 nm using an ultraviolet-visible (UV-Vis) spectrophotometer. The sample was kept for. The percentage for DPPH-radical scavenging activity of the extract was determined by the following formula:

$$\text{Percentage Inhibition } (\%) = \frac{\text{Blank absorbance} - \text{Sample absorbance}}{\text{Blank absorbance}} * 100$$

Extract IC_{50} was measured using linear regression equation y = 0.253x (R^2 = 0.9232) by drawing graph between absorbance verses concentration.

5.6 Experimental animals

Wistar albino rats weighing 180–200 grams were purchased from the Animal House of the University of Agriculture, Faisalabad. They were kept in an animal house (under standard laboratory conditions; room temperature: 25 °C, 12 hours light and dark cycle, humidity 60%) of Govt. College University, Faisalabad for one week before the start of the experiment to acclimatize the animals. They had free access to food and water.

5.7 Ethical approval for animal studies

The *in vivo* study was executed after getting ethical approval from Institutional Review Board (Reference No. GCUF/ERC/2035; 25-1-2019) ruled under the regulation of the Institute of Laboratory Animal Resources, Commission on Life Sciences University, National Research Council (1996).

5.8 Study design

Thirty-six healthy rats of both sexes were divided into 6 groups (n = 6). Group I was normal to control (NCG), to whom the vehicle was given orally. Group II served as disease control (DCG), receiving haloperidol 1 mg/kg intraperitoneally [71, 72]. Group III was the standard group, received L-Dopa 100 mg/kg + carbidopa 25 mg/kg orally. Groups IV–VI treatment groups received extract at 200, 400, and 600 mg/kg dose levels respectively via the oral route. All the groups were given their relevant treatments for 21 days using a gavage needle.

Behavioral evaluation of the NCG was started from day one whereas in other groups behavioral observations were started from the eighteenth day of the study to evaluate the anti-PD effect of the extract.

On the 22nd day, all the animals were humanely killed by cervical dislocation under mild chloroform anesthesia. Brains were excised from all the animals for biochemical and histopathological analyses to examine the anti-PD effect of the plant extract. For the preparation of tissue homogenate (10%w/v) and biochemical assays brain was isolated and the homogenate was prepared with phosphate buffer.

5.9 Evaluation of anti-Parkinson activity (in vivo study)

5.9.1 Behavioral studies

To observe the effect of plant extract on motor functions of rats with haloperidol-induced Parkinsonism, various types of behavioral tests were employed.

5.9.1.1 Catalepsy test

The catalepsy test was performed to evaluate the muscle's rigidity. The bar has 1 cm diameter and 3 cm highest from the floor was used in the experiment. Rat's forelimbs were placed on the bar and time was recorded in which rats step down from the bar. The time at which the animals fall was considered as cataleptic time (seconds). This test was carried out on the 7th, 14th and 21st day of the study [73, 74].

5.9.1.2 Hang test

In the grid hang test neuromuscular strength was determined. This test was carried out on the 7th, 14th, and 21st days during the study. Rats were picked up from their tails and steadily put down on a straight gauze and hold up until they snatched the gauze with their front and hind paws. The gauze was then upturned so that the rats were allowed to hang upside down. The gauze was ascended 20 cm overhead a solid surface, to depress the falling but not become the cause of any injury if the rat falls. The reading was taken on a stopwatch after 30 seconds when the rats fell [74].

5.9.1.3 Horizontal bar test

Muscle coordination was checked in this test. The apparatus comprised of a bar (brass material) 38 cm in length that was held with wooden support up to 49 cm high from the surface. Bars of three diameters (2, 4, and 6 mm) were used to assess coordination. This test was carried out on the 7th, 14th, and 21st days. Rats were held by their tails and put down on the bench in front of the apparatus. They were slipped quickly backward at least 20 cm when rats gripped the bar with their forepaw, their tails were left. Time was noted with the stopwatch to record how long a rat takes to fall on the ground. The utmost break-off time was 30 seconds [75].

5.9.2 Biochemical analysis of brain

Brains tissue homogenate (10%w/v) was prepared in 0.1 M (Ph 7.4) phosphate buffer using automated tissue homogenizer for estimation of SOD, catalase, lipid peroxidation, and GSH to sort out the anti-PD effect of the extract on these organs.

The total protein contents were estimated by adopting the previously followed method. Briefly, the absorbance of the reaction mixture was taken at 660 nm using a UV-Vis spectrophotometer. Standard curve of bovine serum was used for the expression analysis of the protein levels were expressed in mg/mL [5].

5.9.2.1 Estimation of Superoxide dismutase (SOD) activity

0.1M potassium phosphate buffer (pH 7.4) (2.8 mL) and 0.1 mL tissue homogenate and pyrogallol solution (500 mg pyrogallol in 2 mL water + 12 g potassium hydroxide in 8 mL water) were mixed in a test tube. Absorbance was taken at 325 nm [5].

5.9.2.2 Estimation of catalase (CAT) Levels

For CAT activity, the reaction mixture was contained 0.05 mL of sample, 1.95 mL of phosphate buffer (50 Mm; pH 7), and 1mL of H_2O_2 (30 mM) solution. The absorbance was measured at 240 nm [76]. Micromoles of H_2O_2 per min per mg was used as an expression of CAT levels. The cat activity was calculated by using the following formula:

$$\text{CAT activity } = \text{OD/E} \times \text{ vol of sample } \times \text{mg of protein}$$

5.9.2.3 Estimation of Malondialdehyde (MDA) level

For determining lipid peroxidation in tissue homogenate of treated animals, malondialdehyde level was estimated which is an indirect method by following earlier procedure. In this test, 1 mL of the sample and 3 mL thiobarbituric acid (TBA; 0.38% w/w) was taken in a test tube, mixed properly followed by holding on an ice bath for 15 min. Afterward, centrifugation at 3000 rpm was done for 10 min. The absorbance of the upper layer was taken at 532 nm. The concentration of MDA was calculated by using the following formula.

$$\text{MDA concentraion } = \frac{\text{ABS532} \times 100 \times \text{VT}}{1.56 \times 10^5 \times \text{W} \times \text{VU}}$$

ABS 532 = absorbance; VT = total volume of mixture; VU = Volume of aliquot

1.56×10^5 = molar extinction co-efficient; WT = weight of organ [77].

5.9.2.4 Estimation of reduced glutathione (GSH) level

In this assay, 1 mL of tissue homogenate (10%w/v) was precipitated with 1 mL of 10% trichloroacetic acid (TCA). The aliquot of the supernatant was added with 4 mL of phosphate solution and 0.5 mL of DTNB (5,5-dithiobis-2-nitrobenzoic acid) reagent. The sulfhydryl group of glutathione reacts with DTNB and produces a yellow-colored 5-thio-2-nitrobenzoic acid (TNB). The absorbance of the solution was measured at 412 nm. GSH is determined by using the following formula.

$$\text{GSH} = \text{Y} - \frac{0.00314}{0.034} \times \text{DF/T} \times \text{VU}$$

DF = Dilution Factor; VU = Volume of aliquot

Y = Absorbance at 412 nm; T = Tissue homogenate [76].

5.9.2.5 Estimation of dopamine levels

For the estimation of dopamine, HCI-butanol was used for the preparation of brain tissue homogenate. The reaction mixture was then centrifuged at 2000 rpm for 10 minutes. In 1 mL of supernatant, 2.5 mL heptane and 0.3 mL (0.1M HCI) were added and centrifuged at 2000 rpm for 10 minutes. Remove the aqueous layer and in a 0.2 mL of layer, 0.05 mL (0.4 M HCI) and 0.1 mL of EDTA were added. For the start of oxidation, 0.1 mL of iodine solution was added. Sodium sulphite (0.1 mL) and 0.1 mL of acetic acid were added to the reaction mixture to stop the oxidation reaction. The reaction mixture was heated at 100 °C

for 6 minutes. The absorbance of the reaction mixture was measured at 350nm. The regression line of dopamine was used for the estimation of dopamine levels in brain tissue [78].

5.9.2.6 Estimation of MAO-B levels

In a 250 μL of serotonin and buffer, brain tissue homogenate (250 μL) was added and incubated the mixture at 37 °C for 20 minutes. 1M HCI (200 μL) was added to arrest the reaction then 5 mL cyclohexane was added and the organic phase was removed and absorbance was taken out at 242 nm. In a blank 1M HCI was added before the serotonin and buffer [33]. Levels of MAO-B were calculated by using the following formula:

$$X = \text{Sample } (abs) - \text{Blank}(abs) \times \text{Conc.of Standard} \div \text{Standard } (abs) - \text{Blank } (abs)$$

5.9.3 Histopathology analysis

The isolated brains were preserved in 10% formalin solution and the slides were prepared for microscopic evaluation. Digital images were captured using an optical microscope under the polarized light.

5.10 Molecular docking analysis

Molecular docking assists to understand and visualize the binding interactions of extracted phytochemicals with the enzyme acetylcholine-esterase, which is one of the remarkable drug targets for PD [79]. For the analysis of protein-ligand interactions, preliminary requirements were the three-dimensional structure of protein and ligand dataset, X-rays crystallographic structure of AChE protein with PDB ID: 4EY7 with the resolution of 2.35 Å was used for molecular docking interpretations [80]. While 12 phytochemicals; pyrogallol (CID: 1057), gallic acid (CID: 370), catechol (CID: 289), catechin (CID: 73160), hydroxybenzoic acid (CID: 135), chlorogenic acid (CID: 1794427), caffeic acid (CID: 689043), sinapic acid (CID: 637775), coumaric acid (CID: 637542), ferulic acid (CID: 445858), rutin (CID: 5280805) and sinigrin (CID: 6911854) in three-dimensional conformations were downloaded from PubChem database [35]. Molecular Operating Environment (MOE) software package (version 2016.10 Chemical Chemical Computing Group Montreal, Quebec, Canada) was used for molecular docking of AchE protein with selected 12 phytochemicals. The chemical structures were directed to the system to prepare and optimize the files before the docking procedure. The integral issues were found in the co-crystallized macromolecule and corrected, missing residues were added, the irrelevant molecular moieties such as water elements, co-factor, ions were removed. Polar hydrogen atoms were added. The protonate function was applied for the optimization. By using the Dock module of MOE, molecular docking was performed, the native binding site was identified from the co-crystallized protein structure. The energy minimization was done by the Amber: 10EHT force field. The triangular matcher placement method was selected with the London dG scoring function. The initially docked poses were refined by the induced-fit docking protocols and selected the GBVI/WSA dG scoring function. Docked complex with the lowest binding energies/highest binding affinities was subjected for interaction analysis.

5.11 Pharmacokinetics and toxicity risk assessment

In silico pharmacokinetic parameters were evaluated by the SwissADME web tool (http://www.swissadme.ch/), major properties calculated were medicinal chemistry-related parameters such as pharmacokinetics, lipophilicity, water-solubility, drug-likeness, identification of undesirable structural moieties, and toxicity alerts of the selected phytochemicals. Osiris property explorer (https://www.organic-chemistry.org/prog/peo/) was used to estimate the toxicity on the four major grounds such as tumorigenic, irritant, mutagenic, and reproductive properties. It also calculated the drug-likeness and drug score, which explains the ADMET (absorption, distribution, metabolism, elimination, and toxicity) profile of the extracted phytochemicals as explained in our previous study [32].

5.12 Statistical analysis

Results were expressed as the mean ± S.E.M. the data was analyzed by the application of two-way ANOVA followed by the Bonferroni test by the GraphPad prism (version 5.0, GraphPad Software, San Diego, California USA), the value of $p < 0.05$ was set as the statistical significant parameter value.

6. Conclusions

Parkinson's disease (PD) is the most frequent neurodegenerative disease in an older population. Plants have been the backbone of the development of treatment options for acute to chronic diseases. In this study, we have studied and established the therapeutic potential of *Brassica juncea* in PD. Molecular docking analysis explains the protein-ligand interactions of the selected 12 phytochemicals and concluded with the four best results of sinapic acid, rutin, ferulic acid, and caffeic acid within the active binding site of AChE target protein, and ADMET profile estimations also supported the selection of potential compounds. *Brassica juncea* improved motor functions and enhanced the antioxidant enzymes in brain tissues. *B. juncea* at 600 mg/kg dose level highly significantly improved the locomotion and neurotransmitters levels. *B. juncea* at the same dose significantly reduced the MAO-B levels in the brain that means the breakdown of dopamine is inhibited significantly. Hence, it is estimated that *B. Juncea* and its extracted metabolites could be efficacious for the treatment of PD and further development in this regard may provide us with effective and potential treatment.

7. Author contributions

US, MAS, BA, GMS conceived and designed the experiments; SB, MSK, HM, MQ NJ, SH performed the experiments and MFA, AS, ZC, FA, RHA analyzed the data; MA, MAA, RB, CV, OH, RHA contributed reagents and materials.

8. Ethics approval and consent to participate

The experimental protocol involving the caring, handling, and treatment of rats for the experiment was approved by the Government College University Faisalabad, Pakistan Institutional Review Board (GCUF/ERC/2035).

9. Acknowledgment

The authors would like to extend their sincere appreciation to Taif University Researchers Supporting Project number (TURSP-2020/309), Taif University, Taif, Saudi Arabia.

10. Funding

Taif University Researchers Supporting Project number (TURSP-2020/309), Taif University, Taif, Saudi Arabia.

11. Conflict of interest

The authors declare no conflict of interest.

12. References

[1] Banu Z, Fatima SJ, Fatima A, Fatima S, Zohra SF, Sultana T. Phytochemical Evaluation and Pharmacological Screening of Antiparkinson's Activity of Allium Sativum In Swiss/Albino Mice. IOSR Journal of Pharmacy, 2016; 6: 1–12.

[2] Saleem U, Gull Z, Saleem A, Shah MA, Akhtar MF, Anwar F, *et al*. Appraisal of anti-Parkinson activity of rhinacanthin-C in haloperidol-induced parkinsonism in mice: a mechanistic approach. Journal of Food Biochemistry. 2021; 45: e13677.

[3] Chin-Chan M, Navarro-Yepes J, Quintanilla-Vega B. Environmental pollutants as risk factors for neurodegenerative disorders: Alzheimer and Parkinson diseases. Frontiers in Cellular Neuroscience. 2015; 9: 124.

[4] Postuma RB, Berg D, Stern M, Poewe W, Olanow CW, Oertel W, *et al*. MDS clinical diagnostic criteria for Parkinson's disease. Movement Disorders. 2015; 30: 1591–1601.

[5] Bhangale JO, Acharya SR. Anti-Parkinson Activity of Petroleum Ether Extract ofFicus religiosa Leaves. Advances in Pharmacological Sciences. 2016; 2016: 1–9.

[6] Ascherio A, Schwarzschild MA. The epidemiology of Parkinson's disease: risk factors and prevention. The Lancet Neurology. 2016; 15: 1257–1272.

[7] Skorvanek M, Goldman JG, Jahanshahi M, Marras C, Rektorova I, Schmand B, *et al*. Global scales for cognitive screening in Parkinson's disease: Critique and recommendations. Movement Disorders. 2019; 33: 208–218.

[8] Poewe W, Antonini A. Novel formulations and modes of delivery of levodopa. Movement Disorders. 2015; 30: 114–120.

[9] Souilah N, Bendif H, Ullah Z, Miara MD, Laib M, Öztürk M, *et al*. LC-MS/MS Profiling of 37 Fingerprint Phytochemicals in Oenanthe fistulosa L. and its Biological Activities. The Natural Products Journal. 2021; 11: 63–73.

[10] Jothilin Subitsha A, Khanam S, Sabu S. Plants as a promising source for the treatment of parkinson disease: a systemic review. IP International Journal of Comprehensive and Advanced Pharmacology. 2021; 5: 158–166.

[11] Khan ST, Ahmed S, Gul S, Khan A, Al-Harrasi A. Search for safer and potent natural inhibitors of Parkinson's disease. Neurochemistry International. 2021; 149: 105135.

[12] Bawani SS, Anandhi DU. GC-MS Analysis of Nigella Sativa Seed Extract and Its Ameliorative Effects on Transgenic Drosophila Model of Parkinson Disease. International Journal of Innovative Science and Research Technology. 2021; 4: 16–22.

[13] Iuvone T, De Filippis D, Esposito G, D'Amico A, Izzo AA. The Spice Sage and its Active Ingredient Rosmarinic Acid Protect PC12 Cells from Amyloid-β Peptide-Induced Neurotoxicity. Journal of Pharmacology and Experimental Therapeutics. 2006; 317: 1143–1149.

[14] Nah JJ, Hahn JH, Chung S, Choi S, Kim YI, Nah SY. Effect of ginsenosides, active components of ginseng, on capsaicin-induced pain-related behavior. Neuropharmacology. 2000; 39: 2180–2184.

[15] Nah SY, Park HJ, McCleskey EW. A trace component of ginseng that inhibits Ca2+ channels through a pertussis toxin-sensitive G protein. Proceedings of the National Academy of Sciences. 1995; 92: 8739–743.

[16] Berk M, Post R, Ratheesh A, Gliddon E, Singh A, Vieta E, *et al*. Staging in bipolar disorder: from theoretical framework to clinical utility. World Psychiatry. 2019; 16: 236–44.

[17] de Sousa ASB, da Silva MCA, Lima RP, Meireles BRLDA, Cordeiro ATM, Santos EFDS, *et al*. Phenolic compounds and antioxidant activity as discriminating markers and adding value of mango varieties. Scientia Horticulturae. 2021; 287: 110259.

[18] Naveen K, Bhattacharjee. Medicinal Herbs As Neuroprotective Agents. World Journal of Pharmacy and Pharmaceutical Sciences 2021; 4: 675–689.

[19] Baenas N, González-Trujano ME, Guadarrama-Enríquez O, Pellicer F, García-Viguera C, Moreno DA. Broccoli sprouts in analgesia - preclinical *in vivo* studies. Food & Function. 2018; 8: 167–176.

[20] Sharma A, Kumar V, Kanwar M, Thukral A and Bhardwaj R. Phytochemical profiling of the leaves of Brassica juncea L. using GC-MS. International Food Research Journal. 2017; 24: 547.

[21] Kumar V, Thakur AK, Barothia ND, Chatterjee SS.Therapeutic potentials of Brassica juncea: an overview. Tang [Humanitas Medicine]. 2011; 1: 1–16.

[22] Alam MB, Hossain MS, Haque ME. Antioxidant and anti-inflammatory activities of the leaf extract of Brassica nigra. Journal of Applied Pharmaceutical Science. 2011; 2: 303.

[23] Björkman M, Klingen I, Birch ANE, Bones AM, Bruce TJA, Johansen TJ, *et al*. Phytochemicals of Brassicaceae in plant protection and human health–influences of climate, environment and agronomic practice. Phytochemistry. 2011; 72: 538–556.

[24] Yu JC, Jiang ZT, Li R, Chan SM. Chemical Composition o f the Essential Oils of Brassica juncea (L) CossGrown in Different Regions, Hebei, Shaanxi and Shandong, of China. Journal of Food and Drug Analysis. 2003; 1: 22–26.

[25] Avato P, Argentieri MP. Brassicaceae: a rich source of health improving phytochemicals. Phytochemistry Reviews. 2015; 14: 1019–1033.

[26] Yadav AK, Thakur J, Prakash O, Khan F, Saikia D, Gupta MM. Screening of flavonoids for antitubercular activity and their structure–activity relationships. Medicinal Chemistry Research. 2013; 22: 2706–2716.

[27] Krumbein A, Schonhof I, Schreiner M. Composition and contents of phytochemicals (glucosinolates, carotenoids and chlorophylls) and ascorbic acid in selected Brassica species (B. juncea, B. rapa subsp. nipposinica var. chinoleifera, B. rapa subsp. chinensis and B. rapa subsp. rapa). Journal of Applied Botany and Food Quality. 2015; 79: 168–174.

[28] Terstappen GC, Reggiani A. In silico research in drug discovery. Trends in Pharmacological Sciences. 2001; 22: 23–26.

[29] Mishra H, Singh N, Lahiri T, Misra K: A comparative study on the molecular descriptors for predicting drug-likeness of small molecules. Bioinformation. 2009; 3: 384.

[30] Pajouhesh H, Lenz GR. Medicinal chemical properties of successful central nervous system drugs. Neurotherapeutics. 2005; 2: 541–553.

[31] Yang Z, Yang Z, He J, Lu A, Liu S, Hou T, *et al*. Benchmarking the mechanisms of frequent hitters: limitation of PAINS alerts. Drug Discovery Today. 2021; 26: 1353–1358.

[32] Osman W, Ismail EMOA, Shantier SW, Mohammed MS, Mothana RA, Muddathir A, *et al*. In silico assessment of potential leads identified from Bauhinia rufescens Lam. as α-glucosidase and α-amylase inhibitors. Journal of Receptors and Signal Transduction. 2021; 41: 159–169.

[33] Sanawar M, Saleem U, Anwar F, Nazir S, Akhtar MF, Ahmad B, Ismail Y. Investigation of anti-Parkinson activity of dicyclomine. International Journal of Neuroscience. 2020; 9: 1–14.

[34] Saleem U, Gull Z, Saleem A, Shah MA, Akhtar MF, Anwar F, et al. Appraisal of anti-Parkinson activity of rhinacanthin-C in haloperidol-induced parkinsonism in mice: a mechanistic approach. Journal of Food Biochemistry. 2021; 45: e13677.

[35] Saleem U, Shehzad A, Shah S, Raza Z, Shah MA, Bibi S, *et al*. Antiparkinsonian activity of Cucurbita pepo seeds along with possible underlying mechanism. Metabolic Brain Disease. 2021; 36: 1231–1251.

[36] Saleem U, Chauhdary Z, Raza Z, Shah S, Rahman M, Zaib P, *et al*. Anti-Parkinson's Activity of Tribulus terrestris via Modulation of AChE, α-Synuclein, TNF-α, and IL-1β. ACS Omega. 2020; 5: 25216–25227.

[37] Saleem U, Raza Z, Anwar F, Chaudary Z, Ahmad B. Systems pharmacology based approach to investigate the in-vivo therapeutic efficacy of Albizia lebbeck (L.) in experimental model of Parkinson's disease. BMC Complementary and Alternative Medicine. 2019; 19: 352.

[38] De La Cruz JP, Ruiz-Moreno MI, Guerrero A, López-Villodres JA, Reyes JJ, Espartero JL, *et al*. Role of the catechol group in the antioxidant and neuroprotective effects of virgin olive oil components in rat brain. The Journal of Nutritional Biochemistry. 2016; 26: 549–555.

[39] Napolitano A, Cesura AM, Da Prada M. The role of monoamine oxidase and catechol O-methyltransferase in dopaminergic neurotransmission. Journal of Neural Transmission. Supplementum. 1996; 45: 35–45.

[40] Oliveira C, Cagide F, Teixeira J, Amorim R, Sequeira L, Mesiti F, *et al*. Hydroxybenzoic Acid Derivatives as Dual-Target Ligands: Mitochondriotropic Antioxidants and Cholinesterase Inhibitors. Frontiers in Chemistry. 2019; 6: 126.

[41] Winter AN, Brenner MC, Punessen N, Snodgrass M, Byars C, Arora Y, *et al*. Comparison of the Neuroprotective and Anti-Inflammatory Effects of the Anthocyanin Metabolites, Protocatechuic Acid and 4-Hydroxybenzoic Acid. Oxidative Medicine and Cellular Longevity. 2018; 2017: 6297080.

[42] Ola MS, Ahmed MM, Ahmad R, Abuohashish HM, Al-Rejaie SS, Alhomida AS. Neuroprotective Effects of Rutin in Streptozotocin-Induced Diabetic Rat Retina. Journal of Molecular Neuroscience. 2015; 56: 440–448.

[43] Pu F, Mishima K, Irie K, Motohashi K, Tanaka Y, Orito K, *et al*. Neuroprotective effects of quercetin and rutin on spatial memory impairment in an 8-arm radial maze task and neuronal death induced by repeated cerebral ischemia in rats. Journal of Pharmacological Sciences. 2007; 104: 329–334.

[44] Liu Q, Li X, Ouyang X, Chen D. Dual Effect of Glucuronidation of a Pyrogallol-Type Phytophenol Antioxidant: A Comparison between Scutellarein and Scutellarin. Molecules. 2018; 23: 3225.

[45] Verzelloni E, Pellacani C, Tagliazucchi D, Tagliaferri S, Calani L, Costa LG, *et al*. Antiglycative and neuroprotective activity of colon-derived polyphenol catabolites. Molecular Nutrition & Food Research. 2011; 55: S35-S43.

[46] Lu Z, Nie G, Belton PS, Tang H, Zhao B. Structure-activity relationship analysis of antioxidant ability and neuroprotective effect of gallic acid derivatives. Neurochemistry International. 2006; 48: 263–274.

[47] Mansouri MT, Farbood Y, Sameri MJ, Sarkaki A, Naghizadeh B, Rafeirad M. Neuroprotective effects of oral gallic acid against oxidative stress induced by 6-hydroxydopamine in rats. Food Chemistry. 2013; 138: 1028–1033.

[48] Shabani S, Rabiei Z, Amini-Khoei H. Exploring the multifaceted neuroprotective actions of gallic acid: a review. International Journal of Food Properties. 2020; 23: 736–752.

[49] Mandel S, Youdim MBH. Catechin polyphenols: neurodegeneration and neuroprotection in neurodegenerative diseases. Free Radical Biology and Medicine. 2005; 37: 304–317.

[50] Kumar G, Mukherjee S, Paliwal P, Singh SS, Birla H, Singh SP, *et al*. Neuroprotective effect of chlorogenic acid in global cerebral ischemia-reperfusion rat model. Naunyn-Schmiedeberg's Archives of Pharmacology. 2019; 392: 1293–1309.

[51] Jeong C, Jeong HR, Choi GN, Kim D, Lee U, Heo HJ. Neuroprotective and anti-oxidant effects of caffeic acid isolated from Erigeron annuus leaf. Chinese Medicine. 2011; 6: 25.

[52] Chen C. Sinapic Acid and its Derivatives as Medicine in Oxidative Stress-Induced Diseases and Aging. Oxidative Medicine and Cellular Longevity. 2016; 2016: 3571614.

[53] Guven M, Aras AB, Akman T, Sen HM, Ozkan A, Salis O, *et al*. Neuroprotective effect of p-coumaric acid in rat model of embolic cerebral ischemia. Iranian Journal of Basic Medical Sciences. 2015; 18: 356–363.

[54] Cheng C, Su S, Tang N, Ho T, Chiang S, Hsieh C. Ferulic acid provides neuroprotection against oxidative stress-related apoptosis after cerebral ischemia/reperfusion injury by inhibiting ICAM-1 mRNA expression in rats. Brain Research. 2008; 1209: 136–150.

[55] Hira S, Saleem U, Anwar F, Ahmad B. Antioxidants Attenuate Isolation- and L-DOPA-Induced Aggression in Mice. Frontiers in Pharmacology. 2019; 8: 945.

[56] Sunday O, Temitope O, Adekunle M, Elizabeth O, Olufunminyi A, Richard A, *et al*. Alteration in antioxidants level and lipid peroxidation of patients with neurodegenerative diseases Alzheimer's disease and Parkinson disease. International Journal of Nutrition, Pharmacology, Neurological Diseases. 2014; 4: 146.

[57] Saleem U, Akhtar R, Anwar F, Shah MA, Chaudary Z, Ayaz M, *et al*. Neuroprotective potential of Malva neglecta is mediated via down-regulation of cholinesterase and modulation of oxidative stress markers. Metabolic Brain Disease. 2021; 36: 889–900.

[58] Parambi DGT, Saleem U, Shah MA, Anwar F, Ahmad B, Manzar A, *et al*. Exploring the Therapeutic Potentials of Highly Selective Oxygenated Chalcone Based MAO-B Inhibitors in a Haloperidol-Induced Murine Model of Parkinson's Disease. Neurochemical Research. 2020; 45: 2786–2799.

[59] Hira S, Saleem U, Anwar F, Raza Z, Rehman AU, Ahmad B. In Silico Study and Pharmacological Evaluation of Eplerinone as an Anti-Alzheimer's Drug in STZ-Induced Alzheimer's Disease Model. ACS Omega. 2020; 5: 13973–13983.

[60] Girotti AW. Mechanisms of lipid peroxidation. Journal of Free Radicals in Biology & Medicine. 1986; 1: 87–95.

[61] Halliwell B, Chirico S. Lipid peroxidation: its mechanism, measurement, and significance. The American Journal of Clinical Nutrition. 1993; 57: 715S–724S.

[62] Niki E, Yoshida Y, Saito Y, Noguchi N. Lipid peroxidation: mechanisms, inhibition, and biological effects. Biochemical and Biophysical Research Communications. 2005; 338: 668–676.
[63] Li N, Jiang H, Yang J, Wang C, Wu L, Hao Y, *et al*. Characterization of phenolic compounds and anti-acetylcholinase activity of coconut shells. Food Bioscience. 2021; 42: 101204.
[64] Bourdon AK, Villareal G, Perry G, Phelix CF. Alzheimer's and Parkinson's Disease Novel Therapeutic Target. International Journal of Knowledge Discovery in Bioinformatics. 2017; 7: 68–82.
[65] Sang-Bin L,Yang HO. Neuroprotective effect of sinapic acid on REV-ERB α modulated mitochondrial fission in Parkinson's disease. Authorea Preprints 2020; 8: 1–18.
[66] Lee HE, Kim DH, Park SJ, Kim JM, Lee YW, Jung JM, *et al*. Neuroprotective effect of sinapic acid in a mouse model of amyloid β(1-42) protein-induced Alzheimer's disease. Pharmacology, Biochemistry, and Behavior. 2013; 103: 260–266.
[67] Moreton RC. United States pharmacopeia-national formulary. Journal of Excipients and Food Chemicals. 2016; 6: 925.
[68] Das B, Moumita S, Ghosh S, Khan MI, Indira D, Jayabalan R, *et al*. Biosynthesis of magnesium oxide (MgO) nanoflakes by using leaf extract of Bauhinia purpurea and evaluation of its antibacterial property against Staphylococcus aureus. Materials Science and Engineering. C, Materials for Biological Applications. 2018; 91: 436–444.
[69] Saleem U, Hussain K, Ahmad M, Irfan Bukhari N, Malik A, Ahmad B. Physicochemical and phytochemical analysis of Euphorbia helioscopia (L.). Pakistan journal of pharmaceutical sciences. 2014; 3: 577–585.
[70] Jamshed H, Siddiqi HS, Gilani AH, Arslan J, Qasim M, Gul B. Studies on antioxidant, hepatoprotective, and vasculoprotective potential of Viola odorata and Wrightia tinctoria. Phytotherapy Research. 2019; 33: 2310–2318.
[71] Duty S, Jenner P. Animal models of Parkinson's disease: a source of novel treatments and clues to the cause of the disease. British Journal of Pharmacology. 2012; 164: 1357–1391.
[72] Pemminati S, Nair V, Dorababu P, Gopalakrishna H, Pai M. Effect of ethanolic extract of leaves of Ocimum sanctum on haloperidol-induced catalepsy in albino mice. Indian Journal of pharmacology. 2007; 39: 87–89.
[73] Ahmed HH, Abdel-Rahman M, Ali RS, Abdel Moniem A. Protective effect of Ginkgo biloba extract and pumpkin seed oil against neurotoxicity of rotenone in adult male rats. The Journal of Applied Sciences Research. 2009; 5: 622–635.
[74] Barroca NCB, Guarda MD, da Silva NT, Colombo AC, Reimer AE, Brandão ML, *et al*. Influence of aversive stimulation on haloperidol-induced catalepsy in rats. Behavioural Pharmacology. 2019; 30: 229–238.
[75] Fischer R, Maier O. Interrelation of Oxidative Stress and Inflammation in Neurodegenerative Disease: Role of TNF. Oxidative Medicine and Cellular Longevity. 2015; 2015: 1–18.
[76] Thonda V, Kumar SH, Handral M, Sonowal A. Neuroprotective evaluation of ethanolic leaf extract of Dalbergia sissoo in monosodium glutamate induced neurotoxicity in rats. International Journal of Pharmaceutical Sciences and Research. 2014; 5: 829–838.
[77] Swaroop T, Handral S, Mitul P. Neuroprotective evaluation of Dalbergia sissoo roxb. leaves against cerebral ischemia/reperfusion (I/R) induced oxidative stress in rat. Indo American Journal of Pharmaceutical Research. 2013; 3: 3689–3701.
[78] S. Nazir, F. Anwar, U. Saleem, B. Ahmad, Z. Raza, M. Sanawar, A. ur Rehman and T. Ismail: Drotaverine Inhibitor of PDE4: Reverses the Streptozotocin Induced Alzheimer's Disease in Mice. Neurochemical research. 2021; 7: 1814–1829.
[79] Zhang P, Xu S, Zhu Z, Xu J. Multi-target design strategies for the improved treatment of Alzheimer's disease. European Journal of Medicinal Chemistry. 2019; 176: 228–247.
[80] Cheung J, Rudolph MJ, Burshteyn F, *et al*. Structures of human acetylcholinesterase in complex with pharmacologically important ligands. Journal of medicinal chemistry, 2012, 55: 10282–10286.

Keywords: Antioxidant; Molecular docking; Neuronal dysfunction; Oxidative stress; Haloperidol; Dopamine

Send correspondence to:

Uzma Saleem, Department of Pharmacology, Faculty of Pharmaceutical Sciences, Government College University, 38000 Faisalabad, Pakistan, E-mail: uzma95@gmail.com

Muhammad Ajmal Shah, Department of Pharmacognosy, Faculty of Pharmaceutical Sciences, Government College University, 38000 Faisalabad, Pakistan, E-mail: ajmalshah@gcuf.edu.pk